

การขึ้นรูปเลนส์ฟิสิกส์ที่ควบคุมความโค้งได้อย่างแม่นยำ

ด้วยเทคนิคการหยดแบบตรงที่จำกัดขอบเขต

นางสาวณัฐนันท์ แก้วมณี

จุฬาลงกรณ์มหาวิทยาลัย  
CHULALONGKORN UNIVERSITY

บทคัดย่อและแฟ้มข้อมูลฉบับเต็มของวิทยานิพนธ์ตั้งแต่ปีการศึกษา 2554 ที่ให้บริการในคลังปัญญาจุฬาฯ (CUIR)  
เป็นแฟ้มข้อมูลของนิสิตเจ้าของวิทยานิพนธ์ ที่ส่งผ่านทางบัณฑิตวิทยาลัย

The abstract and full text of theses from the academic year 2011 in Chulalongkorn University Intellectual Repository (CUIR)  
are the thesis authors' files submitted through the University Graduate School.

วิทยานิพนธ์นี้เป็นส่วนหนึ่งของการศึกษาตามหลักสูตรปริญญาวิทยาศาสตรมหาบัณฑิต

สาขาวิชาปิโตรเคมีและวิทยาศาสตร์พอลิเมอร์

คณะวิทยาศาสตร์ จุฬาลงกรณ์มหาวิทยาลัย

ปีการศึกษา 2559

ลิขสิทธิ์ของจุฬาลงกรณ์มหาวิทยาลัย

FABRICATION OF PDMS LENSES WITH PRECISELY CONTROLLED  
CURVATURES BY CONFINED SESSILE DROP TECHNIQUE

Miss Natthanan Kaewmanee



A Thesis Submitted in Partial Fulfillment of the Requirements  
for the Degree of Master of Science Program in Petrochemistry and Polymer Science  
Faculty of Science  
Chulalongkorn University  
Academic Year 2016  
Copyright of Chulalongkorn University

Thesis Title	FABRICATION OF PDMS LENSES WITH PRECISELY CONTROLLED CURVATURES BY CONFINED SESSILE DROP TECHNIQUE
By	Miss Natthanan Kaewmanee
Field of Study	Petrochemistry and Polymer Science
Thesis Advisor	Professor Sanong Ekgasit, Ph.D.
Thesis Co-Advisor	Associate Professor Chuchaat Thammacharoen

---

Accepted by the Faculty of Science, Chulalongkorn University in Partial  
Fulfillment of the Requirements for the Master's Degree

..... Dean of the Faculty of Science  
(Associate Professor Polkit Sangvanich, Ph.D.)

THESIS COMMITTEE

..... Chairman  
(Assistant Professor Warinthorn Chavasiri, Ph.D.)

..... Thesis Advisor  
(Professor Sanong Ekgasit, Ph.D.)

..... Thesis Co-Advisor  
(Associate Professor Chuchaat Thammacharoen)

..... Examiner  
(Associate Professor Kawee Srikulkit, Ph.D.)

..... External Examiner  
(Assistant Professor Wimonlak Sutapun, Ph.D.)

ณัฐนันท์ แก้วมณี : การขึ้นรูปเลนส์พีดีเอ็มเอสที่ควบคุมความโค้งได้อย่างแม่นยำด้วยเทคนิคการหยดแบบตรงที่จำกัดขอบเขต (FABRICATION OF PDMS LENSES WITH PRECISELY CONTROLLED CURVATURES BY CONFINED SESSILE DROP TECHNIQUE) อ.ที่ปรึกษาวิทยานิพนธ์หลัก: ศ. ดร.สนอง เอกสิทธิ์, อ.ที่ปรึกษาวิทยานิพนธ์ร่วม: รศ. ชูชาติ ธรรมเจริญ, 66 หน้า.

งานวิจัยนี้นำเสนอวิธีการแบบใหม่ในการขึ้นรูปเลนส์จากพอลิไดเมทิลไซลอกเซน (พีดีเอ็มเอส) อีลาสโตเมอร์ด้วยเทคนิคการหยดแบบตรงที่จำกัดขอบเขต ทำให้สามารถควบคุมสมบัติของเลนส์ได้อย่างแม่นยำ เช่นความโค้งของเลนส์ ระยะโฟกัส และกำลังขยาย กระบวนการนี้สามารถขึ้นรูปเลนส์พีดีเอ็มเอสได้โดยง่าย รวดเร็ว มีต้นทุนในการผลิตต่ำ ใช้อุณหภูมิในการคงรูปต่ำ และสามารถผลิตในเชิงพาณิชย์ได้ เลนส์พีดีเอ็มเอสอีลาสโตเมอร์ที่ได้มีลักษณะเป็นเลนส์นูนแกมระนาบที่สามารถนำมาติดกับกล้องถ่ายรูปของสมาร์ทโฟนเพื่อเปลี่ยนสมาร์ทโฟนให้เป็นกล้องจุลทรรศน์ดิจิทัลแบบพกพา ในการขึ้นรูปเลนส์พีดีเอ็มเอสสามารถทำได้โดยการหยดพีดีเอ็มเอสเหลวที่มีปริมาตร 3-100 ไมโครลิตร ลงบนฐานแผ่นวงกลมขนาด 2-10 มิลลิเมตร อาศัยความต้านทานต่อการแพร่กระจายของของเหลวโดยขอบคมช่วยในการขึ้นรูปเลนส์พีดีเอ็มเอส ทำให้ส่วนของทรงกลมมีความเสถียรสูงได้ พีดีเอ็มเอสเหลวมีการแพร่กระจายแบบสมมาตรตามทุกทิศทางภายใต้ความสมดุลระหว่างแรงโน้มถ่วงและแรงตึงผิวระหว่างผิวหน้า ทำให้ทรงกลมที่เกิดขึ้นมีความโค้งแน่นอน ในการคงรูปพีดีเอ็มเอสเหลวจะใช้ความร้อนอุณหภูมิ 80 องศาเซลเซียสนาน 30 นาที ทำให้เลนส์พีดีเอ็มเอสที่ได้ไม่มีฟองอากาศอยู่ในตัวเลนส์ มีระยะโฟกัส 3.4-55.2 มิลลิเมตร และมีกำลังขยาย 4.5-73.5 เท่า กระบวนการขึ้นรูปเลนส์นี้สามารถทำซ้ำ กล้องจุลทรรศน์ดิจิทัลสมาร์ทโฟนแบบพกพาสามารถนำไปใช้ถ่ายภาพวัตถุเล็กๆ ที่ไม่สามารถมองเห็นด้วยตาเปล่า เช่นการถ่ายภาพของสิ่งพิมพ์ระดับไมโครเมตร สิ่งตกค้างในการยิงปืนและร่องรอยของกระสุนปืน นอกจากนี้ยังสามารถประยุกต์ใช้ร่วมกับภาพถ่ายแบบพานาโนรามาเพื่อลดความบิดเบือนที่เกิดจากพื้นผิวโค้งของวัตถุ

สาขาวิชา ปีโตรเคมีและวิทยาศาสตร์พอลิเมอร์ ปลายมือชื่อนิติต .....

ปีการศึกษา 2559

ปลายมือชื่อ อ.ที่ปรึกษาหลัก .....

ปลายมือชื่อ อ.ที่ปรึกษาร่วม .....

# # 5771969923 : MAJOR PETROCHEMISTRY AND POLYMER SCIENCE

KEYWORDS: EPDMS LENS, PORTABLE SMARTPHONE DIGITAL MICROSCOPE, THE CONFINED SESSILE DROP

NATTHANAN KAEWMANEE: FABRICATION OF PDMS LENSES WITH PRECISELY CONTROLLED CURVATURES BY CONFINED SESSILE DROP TECHNIQUE. ADVISOR: PROF. SANONG EKGASIT, Ph.D., CO-ADVISOR: ASSOC. PROF. CHUCHAAT THAMMACHAROEN, B.Sc., 66 pp.

This research presented a novel approach for forming lens form elastomeric polydimethylsiloxane (ePDMS) with precisely controlled properties such as curvature, focal length, and magnification via the confined sessile drop technique. This technique is simple, rapid, and cost effective for mass-scale production. The ePDMS lens with plano-convex shape can be directly attached onto a smartphone camera and transform into portable smartphone digital microscope. The fabrication procedure of ePDMS plano-convex lens involved an injection of liquid PDMS (IPDMS) 3-100  $\mu\text{L}$  onto a circular disk with the diameter in the range 2-10 mm. The resistances to spreading by sharp enabled the reproducibility of spherical cap of IPDMS. The IPDMS axisymmetrically spread under the balance between the gravitational force and interfacial tension force for precisely controlled spherical cap. A thermal treatment at 80 °C for 30 min cured the spherical caps IPDMS into a bubble-free solid ePDMS plano-convex lens. The ePDMS plano-convex lens with focal lengths of 3.4-55.2 mm and magnifications of 4.5X-73.5X could be repeatedly reproduced. Portable smartphone digital microscope can be used to capture small objects that cannot be seen with the naked eye such as micro-printing, and gun shoot residue. High-resolution panorama microscope images without distortion were also demonstrated.

Field of Study: Petrochemistry and  
Polymer Science

Academic Year: 2016

Student's Signature .....

Advisor's Signature .....

Co-Advisor's Signature .....

## ACKNOWLEDGEMENTS

I would like to express my deep gratitude to my thesis advisor, Professor Dr. Sanong Ekgasit and my thesis co-advisor, Associate Professor Chuchaat Thammacharoen for guidance, supervision and helpful suggestion throughout the course of this research.

I would like to thank my committee members, Assistant Professor Dr. Warinthorn Chavasiri, Associate Professor Dr. Kawee Srikulkit and Assistant Professor Dr. Wimonlak Sutapun, whose comments have been especially valuable.

I would like to thanks to my friends and colleagues at the Sensor Research Unit (SRU) for the everlasting friendship and technical supports throughout the time of study

Definitely, this research cannot be completed without kindness and helpful of many organizations. First, I would to thanks Program of Petrochemistry and Polymer Science, Chulalongkorn University; Department of chemistry, Faculty of Science, Chulalongkorn University and Scientific and Technological Research Equipment Center, Chulalongkorn University. Special thanks National Research Council of Thailand (NRCT) for financial supports.

Most importantly, I own deep gratitude to my family, especially my father and mother for their love and encouragement.

## CONTENTS

	Page
THAI ABSTRACT .....	iv
ENGLISH ABSTRACT.....	v
ACKNOWLEDGEMENTS .....	vi
CONTENTS.....	vii
LIST OF TABLES .....	ix
LIST OF FIGURES .....	x
LIST OF ABBREVIATIONS.....	xvi
CHAPTER I INTRODUCTION.....	1
1.1 POINT OF CARE TESTING DEVICE .....	1
1.2 SMARTPHONE .....	1
1.3 LAB-ON-PHONE .....	2
1.4 OBJECTIVE OF THE RESEARCH .....	3
1.5 SCOPE OF THE RESEARCH.....	3
1.6 EXPECTED OUTCOME OF THE RESEARCH .....	4
CHAPTER II THEORETICAL BACKGROUND .....	5
2.1 ELASTOMERIC POLYDIMETHYLSILOXANE.....	5
2.1.1 The Composition and Chemical Structure of ePDMS .....	5
2.1.2 Polymerization of the ePDMS.....	7
2.1.3 The Properties of the ePDMS.....	8
2.1.4 Application of the ePDMS .....	9
2.2 ePDMS LENS FABRICATION TECHNIQUE.....	10
2.2.1 The Replica Molding Technique .....	10
2.2.2 The Moldless Surface Energy Minimization Technique.....	11
2.2.3 The Thermal Reflow Process .....	12
2.2.4 The Dielectrophoresis Force Technique.....	13
2.2.5 The Hanging Droplet Technique .....	14
2.2.6 The Inkjet Printing Technique.....	15
CHAPTER III EXPERIMENTAL SECTION.....	17

	Page
3.1 CHEMICALS, MATERIALS, AND INSTRUMENTS .....	17
3.2 FABRICATION PROCEDURES OF ePDMS PLANO-CONVEX LENS .....	18
3.2.1 Preparation of PMMA Circular Disk .....	18
3.2.2 Preparation of IPDMS .....	19
3.3 EFFECT OF EXPERIMENTAL PARAMETERS ON THE FABRICATION OF ePDMS PLANO-CONVEX LENS .....	20
3.3.1 Effect of Circular Disk Material on IPDMS Spreading .....	20
3.3.2 Effects of Drop Position .....	20
3.3.3 Effects of Curing Temperature .....	21
3.3.4 Effects of IPDMS Volume .....	21
3.3.5 Effects of Circular Disk Diameters .....	21
3.3.6 Effects of Circular PDMS Thickness .....	22
3.3.7 Applications of ePDMS Plano-Convex Lens .....	22
3.4 CHARACTERIZATIONS .....	23
3.4.1 Contact Angle .....	23
3.4.2 Focal Length .....	24
3.4.3 Magnification .....	24
3.4.4 Viewing Area .....	25
CHAPTER IV RESULTS AND DISCUSSION .....	26
4.1 PRELIMINARY OBSERVATIONS .....	26
4.2 FABRICATION AND TESTING OF ePDMS PLANO-CONVEX LENSES .....	27
4.3 FIELD APPLICATIONS OF ePDMS PLANO-CONVEX LENSES .....	45
4.4 PANORAMA MICROSCOPE IMAGING BY SMARTPHONE MICROSCOPE .....	47
CHAPTER V CONCLUSIONS .....	53
REFERENCES .....	54
VITA .....	66



## LIST OF TABLES

	<b>Page</b>
Table 2.1     The physical properties of the ePDMS.....	9
Table 2.2     Summary of the technique for ePDMS lens fabrication.....	17



## LIST OF FIGURES

		<b>Page</b>
Figure 2.1	The chemical structure of the ePDMS repeating units.....	6
Figure 2.2	The chemical structure of the ePDMS base.....	6
Figure 2.3	The chemical structure of the ePDMS curing agent.....	7
Figure 2.4	The crosslinking of the ePDMS base: vinyl terminate ends and curing agent: hydrogen terminated ends in the presence of a platinum catalyst.....	7
Figure 2.5	Fabrication of ePDMS micro-lens array by replica molding technique.....	10
Figure 2.6	Fabrication of ePDMS micro-lens array by moldless surface energy minimization technique.....	11
Figure 2.7	Fabrication of ePDMS micro-lens array by thermal reflow process .....	12
Figure 2.8	Fabrication of ePDMS micro-lens array by dielectrophoresis force technique.....	13
Figure 2.9	Fabrication of ePDMS micro-lens array by hanging droplet technique.....	14
Figure 2.10	Fabrication of ePDMS lens by inkjet printing technique.....	15

	<b>Page</b>
Figure 3.1	Photographic images of (A) the laser cutting machine and (B) the PMMA circular disks (with diameter of 2.0, 3.0, 4.0, 5.0, 6.0, 7.0, 8.0, 9.0, and 10.0 mm) used in the fabrication of ePDMS plano-convex lenses..... 18
Figure 3.2	Photographic images of (A) Sylgard <sup>®</sup> 184 and (A) the mixed IPDMS for ePDMS lens fabrication..... 19
Figure 3.3	Photographic image of the contact angle measurement..... 23
Figure 3.4	Photographic image of the focal length measurement..... 24
Figure 3.5	Photographic image of 1-mm square grid paper for viewing area measurement..... 25
Figure 4.1	Time-dependent photographic images of 15- $\mu$ L IPDMS sessile drops axisymmetrically spread on selected flat surfaces of (A) PMMA sheet, (B) PDMS film, (C) PC sheet, and (D) glass slide. Scale bars indicate 2 mm..... 29
Figure 4.2	Photographic image of (A) a bubble-free ePDMS plano-convex lens prepared by the confined sessile drop technique by curing a spherical cap IPDMS on 5-mm PMMA circular disk at 80 °C for 30 min. The ePDMS lens with air bubbles prepared by dispensing a droplet of IPDMS onto a pre-heated (B) 100 °C, (C) 150 °C, and (D) 150 °C glass slide..... 30

	<b>Page</b>
Figure 4.3	Time-dependent images of 15- $\mu$ L IPDMS confined sessile drops spreading on 3-mm PMMA. The droplets were deposited at (A) 0, (B) 0.5, and (C) 1 mm from the center of the disk. Scale bars indicate 1 mm (A-C)..... 33
Figure 4.4	The front side of a new USD 100 banknote show in (A). The red circles indicate arrays of micro-printings. (B-D) show the microscopic images of micro-printing acquired with 3-mm ePDMS plano-convex lenses. (E-G) are the corresponding images with 4X digital zoom. Scale bars indicate 500 $\mu$ m (B-D), and 100 $\mu$ m (E-G)..... 34
Figure 4.5	6-mm ePDMS plano-convex lens of various focal lengths fabricated by dispensing 5, 10, 15, 20, 25, 30, 35, and 40 $\mu$ L IPDMS on 6-mm PMMA disks. The standard deviation (SD) bar of each lens set was calculated from 20 lenses..... 36
Figure 4.6	Microscopic images of the Benjamin Franklin's eyes on the front side of a new USD100 banknote were taken by an iPhone 6s Plus coupled with the 6-mm ePDMS plano-convex lens of various focal lengths fabricated by dispensing (A) 5 $\mu$ L, (B) 10 $\mu$ L, (C) 15 $\mu$ L, (D) 20 $\mu$ L, (E) 25 $\mu$ L, (F) 30 $\mu$ L, (G) 35 $\mu$ L, and (H) 40 $\mu$ L IPDMS. The viewing area (VA, 4:3 format) and contact angle (CA) were indicated in the images... 37

**Page**

- Figure 4.7 Overflow of 45- $\mu$ L IPDMS on a 6-mm PMMA disk. The disk cannot hold the droplet as the local contact angle ( $\theta_P$ ) was much greater than the critical angle for spreading over the edge ( $\theta_C$ ) defined by the Gibbs inequality condition. In this case  $\theta_C=90^\circ$ ..... 38
- Figure 4.8 The ePDMS plano-convex lenses of various focal lengths fabricated by dispensing the highest possible volume of IPDMS on PMMA disks: 2 mm (4  $\mu$ L), 3 mm (6  $\mu$ L), 4 mm (15  $\mu$ L), 5 mm (30  $\mu$ L), 6 mm (40  $\mu$ L), 7 mm (55  $\mu$ L), 8 mm (65  $\mu$ L), 9 mm (80  $\mu$ L), and 10 mm (100  $\mu$ L). The SD bar of each lens set was calculated from 20 lenses..... 40
- Figure 4.9 Microscopic images of George Washington's statue on the flip side of a new USD100 banknote were taken by an iPhone 6s Plus coupled with the ePDMS plano-convex lenses fabricated by dispensing the highest possible volume of IPDMS on PMMA disks: (A) 2 mm (4  $\mu$ L), (B) 3 mm (6  $\mu$ L), (C) 4 mm (15  $\mu$ L), (D) 5 mm (30  $\mu$ L), (E) 6 mm (40  $\mu$ L), (F) 7 mm (55  $\mu$ L), (G) 8 mm (65  $\mu$ L), (H) 9 mm (80  $\mu$ L), and (I) 10 mm (100  $\mu$ L). The viewing area (VA, 4:3 format) and the contact angle (CA) were indicated..... 42

**Page**

- Figure 4.10 Contact angles and curvatures of ePDMS plano-convex lens with diameter of (A) 4 mm, (B) 6 mm, and (C) 8 mm. The contact angles were measured from the images taken by the photographic capability of a standard goniometer (Model 200-F1, Ramé-Hart Instrument Co., USA). The lens curvatures were extracted from the contrast of the images by a MATLAB program. A set of 20 lenses was employed for each diameter. The narrow distributions indicate the reproducibility of the fabrication method..... 42
- Figure 4.11 A set of 100 ePDMS plano-convex lenses (5-mm diameter) fabricated by the confined sessile drop technique and their optical effect when placed on printed characters..... 43
- Figure 4.12 Focal length of 6-mm PDMS elastomeric lens with base of different thickness. Based on the spherical cap fitting, the 6-mm lenses fabricated from a confined sessile drop of 40- $\mu$ L IPDMS have a radius of curvature R of 4.0 mm..... 45
- Figure 4.13 (A) A photographic image of GSRs generate by a point-blank shooting on a cotton fabric. A microscopic image of a GSR taken by (B) normal photography and (C-E) 4X digital zoom. (F) A microscopic image of a clean cotton fabric. The microscope images were captured by an iPhone 6s Plus coupled with a 6-mm ePDMS plano-convex lens..... 47

**Page**

- Figure 4.14 A series of still images show an experiment setup and panorama microscope imaging using a smartphone microscope equipped with a 5-mm ePDMS plano-convex lens and homemade rotating device. The device was rotated at 3 rpm while smartphone microscope taking panorama image of the 3.3 mm x 1.4 mm paper strip wrapped around a 10 mm cylinder. The panorama app stitched the images on-the-fly..... 49
- Figure 4.15 Photographic images of a printed-paper strip as it: (A) was laid on a flat surface and (B) was wrapped around a 10 mm cylinder. (C) Microscopic images of the curved paper strip and (D) the corresponding panorama microscopic image of the curved paper strip taken by an iPhone 6s Plus coupled with a 3-mm lens (see Figure 4.14)..... 50
- Figure 4.16 (A) Photographic images of an FMJ bullet. (B) The corresponding microscopic images of the bullet and (C) panorama microscopic image of the bullet taken by an iPhone 6s Plus coupled with a 3-mm ePDMS plano-convex lens..... 51

## LIST OF ABBREVIATIONS

$^{\circ}\text{C}$	: Degree Celsius
$\phi$	: The subtended angle at the edge
$\mu\text{l}$	: Microliter
$\mu\text{m}$	: Micrometer
$\theta_{\text{C}}$	: The critical contact angle for spreading over the edge
$\theta_{\text{e}}$	: The equilibrium (thermodynamic) contact angle
$\theta_{\text{p}}$	: The local contact angle
POCT	: Point of care testing
CA	: Contact angle
f	: Focal length (mm)
cm	: Centimeter
ePDMS	: Elastomeric polydimethylsiloxane
FMJ	: Full metal jacket
GSRs	: Gunshot residues
h	: High of lens
KPa	: Kilopascal
lPDMS	: Liquid polydimethylsiloxane
M	: Magnification (X)
MEMS	: Microelectromechanic system
min	: Minute
mm	: Millimeter



MPa	: Megapascal
PC	: Polycarbonate
PE	: Polyethylene
PMMA	: Polymethylmethacrylate
R	: Radius of curvature of lens
r	: Radius of lens
rpm	: Rounds per minute
s	: Second
SD	: Standard deviation
SG	: Specific gravity
$T_g$	: Glass transition temperature
$T_m$	: Crystalline melting temperature
VA	: Viewing area

# **CHAPTER I**

## **INTRODUCTION**

### **1.1 POINT OF CARE TESTING DEVICE**

Point of care testing (POCT) device is an instrument using for a simple medical testing or patient care near the testing site and it is operated by physician or healthcare professionals. The advantage of the POCT device is the very fast diagnostic which is allowing the rapid clinical decision making and much better treatments. Nowadays, the development of POCT device are widely practiced [1-9] because of many advantages of this device such as ease of operation and instant response. As a result, physicians or healthcare professionals can instantly take care of their patients. In addition, the POCT devices were demonstrated for the usage in environmental monitoring and food safety analyses [10-11]. Consequently, the researches and developments of the POCT devices are essential for the health of the population and continuous the development of the countries.

### **1.2 SMARTPHONE**

Nowadays, smartphone is a must personal electronic device. The worldwide availability of compact and lightweight smartphones with powerful processor, high quality display, large volume storage, connectivity (3G, 4G, Wi-Fi, Bluetooth, Near Field Communication), ease to use apps, and state-of-the-art sensors (camera,

proximity sensor, magnetometer, accelerometer, gyroscope, microphone, fingerprint sensor, thermometer, and light sensor) at affordable prices was developed. The advanced features of smartphones can be transformed into the future POCT devices. There were 87 million new global subscriptions of mobile phones in the third quarter of 2015 alone. By the end of 2015, the number of mobile phone subscriptions was greater than that of the global population with a greater number of smartphone subscriptions compared to that of the basic phones [12].

### **1.3 LAB-ON-PHONE**

Lab-on-phone devices take advantages of smartphone functionalities such as biosensors [12-21], spectrometer [22-26], and colorimetric sensors [22, 26-31] have been fabricated. Powerful image processing with high pixel density of image sensor encouraged researchers to explore its potential as affordable mobile digital microscope capable of capturing and sharing detailed microscopic images anywhere anytime by attaching an external lens onto the smartphone camera. Various types of lenses including objective lens [32-34], ball lens [34-35], plano-convex lens [20], iPhone lens module [34-36], PDMS elastomeric lens [37-39], and microscope lens [40-42] were employed for coupling the magnified image into the optical system of the smartphone without any hardware modification. The image quality and magnification are strongly depended on the lens and attachment design. Smartphone microscope images with resolution of 1.2  $\mu\text{m}$  by an objective lens [32], 1.5  $\mu\text{m}$  by a plano-convex lens [20], 1.5  $\mu\text{m}$  by a ball lens [35], 1.1  $\mu\text{m}$  by a PDMS elastomeric lens [43], 3.9  $\mu\text{m}$  by a hanging drop PDMS elastomeric lens [37] were successfully acquired.

## 1.4 OBJECTIVE OF THE RESEARCH

This research reveals a simple, rapid, cost effective, and template-free technique for mass-scale production of elastomeric PDMS (ePDMS) plano-convex lens capable of converting a smartphone into a portable digital microscope. The objectives of this research are shown as follows:

- 1.4.1 To develop the confined sessile drop technique for the fabrication of the smartphone compatible plano-convex lens from ePDMS.
- 1.4.2 To investigate the effects of experimental parameters i.e. PDMS drop volume and circular disk diameters on the liquid PDMS (lPDMS) drop profile.
- 1.4.3 To determine the optical properties of and the ePDMS plano-convex lens i.e. curvature, focal length, and magnification.

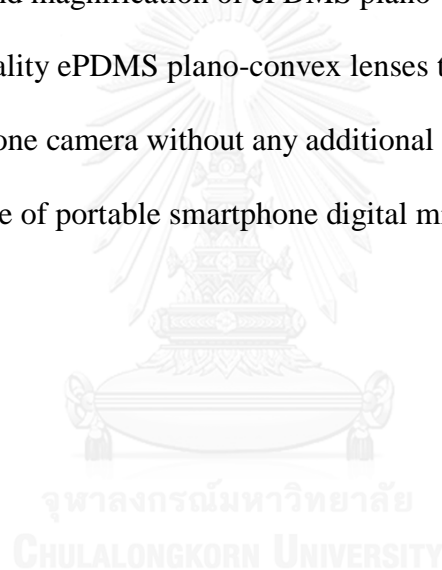
## 1.5 SCOPE OF THE RESEARCH

- 1.5.1 Developing the confined sessile drop technique for fabricating of the ePDMS plano-convex lens from lPDMS under the ambient condition.
- 1.5.2 Controlling parameter of the ePDMS lens i.e. curvature, focal length, and magnification through the varying of experimental parameters i.e. PDMS drop volume, diameter of the substrate, and surface property of the substrate.
- 1.5.3 Comparing the microscopic image quality captured from the ePDMS plano-convex lens attached smartphone and conventional optical microscope.

- 1.5.4 Developing the portable smartphone digital microscope prototype utilizing the ePDMS lens with various magnifications as the objective lens.

## **1.6 EXPECTED OUTCOME OF THE RESEARCH**

- 1.6.1 The fabrication procedure of ePDMS plano-convex lens by the confined sessile drop technique which can precisely control the curvature, focal length and magnification of ePDMS plano-convex lens.
- 1.6.2 High quality ePDMS plano-convex lenses that can be directly attached to smartphone camera without any additional accessories.
- 1.6.3 Prototype of portable smartphone digital microscope.



## CHAPTER II

### THEORETICAL BACKGROUND

#### 2.1 ELASTOMERIC POLYDIMETHYLSILOXANE

Elastomeric polydimethylsiloxane (ePDMS) is the elastomer of silicone which is inexpensive and widely used as sealants, optics, medical devices, and food application [44]. The chemical formula of the ePDMS is  $(\text{CH}_3)_3\text{SiO}[\text{Si}(\text{CH}_3)_2\text{O}]_n(\text{CH}_3)_3$ . The repeating unit of ePDMS is  $[\text{Si}(\text{CH}_3)_2\text{O}]_n$ , where  $n$  is number of repeating units [45]. The ePDMS has many good properties such as highly hydrophobic, colorless, optical transparency, inert, non-toxic, and non-flammable. In fact, the ePDMS lenses can fabricate owing to its optical transparency and non-fluorescence. In addition, the ePDMS lenses can be fabricated in various forms including objective lens [32-34], ball lens [34-35], plano-convex lens [20], iPhone lens module [34-36], ePDMS lens [37-39, 43], and microscope lens [40-42]. The ePDMS lenses were employed for coupling the magnified image into the optical system of the smartphone without any hardware modification.

##### 2.1.1 The Composition and Chemical Structure of ePDMS

The chemical structure of ePDMS composition of silicon, oxygen, carbon, and hydrogen, with siloxane backbone;  $(-\text{Si}-\text{O}-)$  and a  $(\text{Si}(\text{CH}_3)_2\text{O})$  repeating units, as shown in Figure 2.1. The formation of ePDMS (known as Sylgard 184 from

Dow Corning, the pre-polymer of ePDMS) needs two main ingredients consisted of pre-polymer ePDMS base and curing agent. The chemical formula of ePDMS base is  $\text{CH}_2=\text{CH}[\text{Si}(\text{CH}_3)_2\text{O}]_n\text{Si}(\text{CH}_3)\text{CH}=\text{CH}_2$  (where n is the number of repeating units, n ~60), as shown in Figure 2.2 which the ePDMS curing agent is  $\text{CH}_3\text{Si}(\text{CH}_3)_2\text{O}[\text{SiRCHO}]_m\text{SiCH}_3$  (where m is the number of repeating units, n ~10), as shown in Figure 2.3 [46].

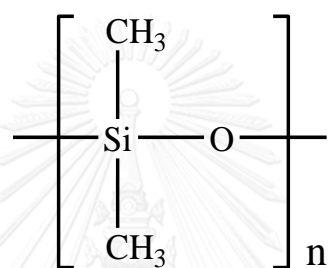


**Figure 2.1** The chemical structure of the ePDMS repeating units.

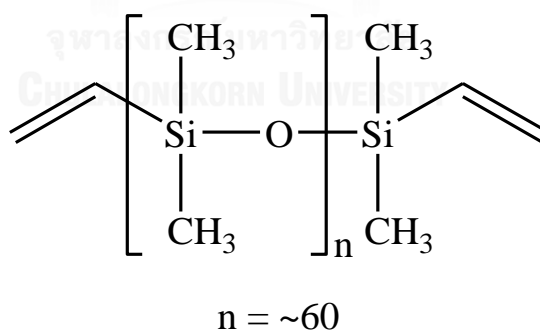
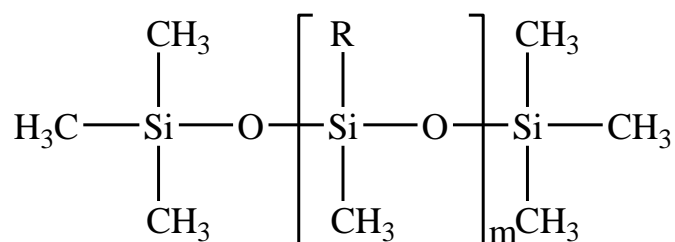


**Figure 2.2** The chemical structure of the ePDMS base.



R is usually CH<sub>3</sub>, sometimes H  
m = ~10

**Figure 2.3** The chemical structure of the ePDMS curing agent.

### 2.1.2 Polymerization of the ePDMS

At room temperature, the ePDMS pre-polymer is a viscous liquid. When the ePDMS base and curing agent are mixed together, the –Si–H bonds of curing agent reacts with the –CH=CH<sub>2</sub> bonds of base and formed –Si–CH<sub>2</sub>–CH<sub>2</sub>–Si– linkages as shown in Figure 2.4. This process is referred to as hydrosilylation of the double bonds. After the complete polymerization and cross-linking, the PDMS material is flexible and highly transparent.

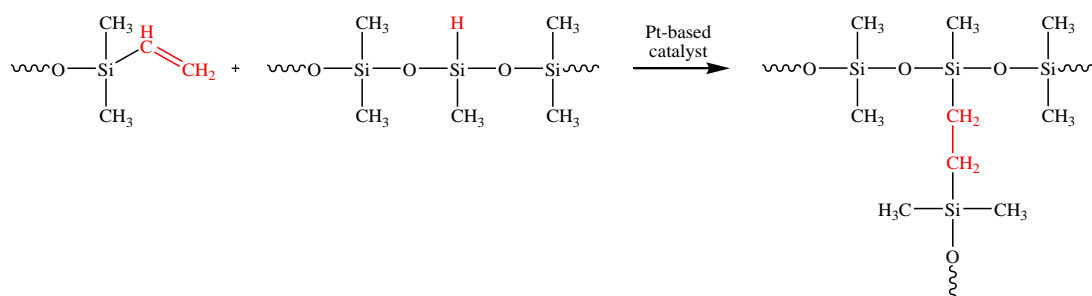


**Figure 2.4** The crosslinking of the ePDMS base: vinyl terminate ends and curing agent: hydrogen terminated ends in the presence of a platinum catalyst.



## 2.1.3 The Properties of the ePDMS

### 2.1.3.1 Physical properties of the ePDMS

The ePDMS is highly transparent, colorless, nontoxic, toughness [47], low glass transition temperature ( $T_g$ ) and crystalline melting temperature ( $T_m$ ). When the surrounding temperature changes over a wide temperatures range from  $-50\text{ }^{\circ}\text{C}$  to  $+200\text{ }^{\circ}\text{C}$ , the ePDMS can remain stability. In addition, the ePDMS will not swell or shrink under high humidity conditions. The ePDMS is large distension. The distended membrane gains full recovery to its original shape. The ePDMS widely used as optics devices (lenses, mirrors, and gratings), microfluidic device, and microelectromechanic system (MEMS) fabrications because the ePDMS is optical transparency from UV to NIR regions and non-fluorescence. The physical properties of ePDMS are shown in Table 2.1.

**Table 2.1** The physical properties of ePDMS

<b>Properties</b>	<b>Value</b>
Refractive Index	1.42
Specific Gravity (SG)	1.03
Glass transition temperature, T <sub>g</sub> (°C)	-125
Crystalline melting temperature, T <sub>m</sub> (°C)	-40
Young's modulus (MPa)	1.2
Shear modulus (KPa)	411
Traction limit (MPa)	1.9
Yield strength (KPa)	700
Compressive modulus (MPa)	2
Poisson Ratio	0.5

### 2.1.3.2 Chemical properties of the ePDMS

The ePDMS is inert. It does not react with water and alcohol. Almost organic solvents can diffuse into the structure of ePDMS which resulted in the swelling of ePDMS. The ePDMS tolerates to extreme temperature, weathering, aging, oxidation, moisture, many chemicals, and ultraviolet radiation because it has highly stable methyl group ( $-\text{CH}_3$ ) [48].

### 2.1.4 Application of the ePDMS

The ePDMS are widely used in many applications such as surfactants and antifoaming, hydraulic fluids and related applications, soft lithography, medicine and cosmetics, skin and hair conditioning, and food processing.

## 2.2 ePDMS LENS FABRICATION TECHNIQUE

### 2.2.1 The Replica Molding Technique

Shih et al., 2006 [49] fabricated ePDMS micro-lens arrays by replica molding technique. The hole of polycarbonate (PC) was formed by the excimer laser and used as substrate. Then, the substrate is coated by spin-coating of liquid poly(methylmethacrylate) (PMMA) and baked at 60 °C for 5 min. After that IPDMS is casted onto the PMMA film. A glass or plastic substrate was covered on IPDMS and baked at 70 °C for 30 min. Finally, the ePDMS micro-lens array was attached by the second replica molding process on the opposite side of substrate. The height of ePDMS micro-lens array in the range of 10-40  $\mu\text{m}$  can be controlled by the diameter of holes PC (50-150  $\mu\text{m}$ ) and the PMMA film thickness can be controlled by speed of spin coating (500-3000 rpm). The ePDMS micro-lens array has highly flat surface and good efficiency in light focusing.

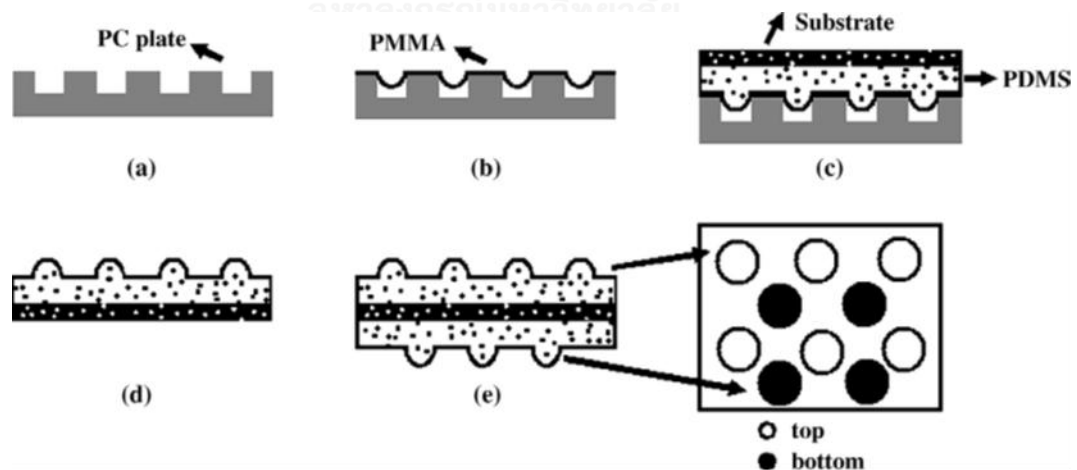


**Figure 2.5** Fabrication of ePDMS micro-lens array by replica molding technique [49].

## 2.2.2 The Moldless Surface Energy Minimization Technique

Cruz-Campa et al., 2010 [50] fabricated ePDMS micro-lens arrays by moldless surface energy minimization technique. The ePDMS micro-lens arrays fabrication procedure was started by an injection of the ePDMS onto controlled temperature preheated surface. In this process, the Engineered Fluid Dispensing™ and MikrosPen™ Accessory for control IPDMS volume were employed. After injecting IPDMS on substrate, the lens was cured at 130 °C for 30 sec and 65 °C for 10 min. The ePDMS micro-lens arrays has focal length in the range 2-25 mm,  $F$ -number in the range 1.4-10, lens diameter in the range 450  $\mu\text{m}$ -4 mm, and lens height in the range 14-600  $\mu\text{m}$ .

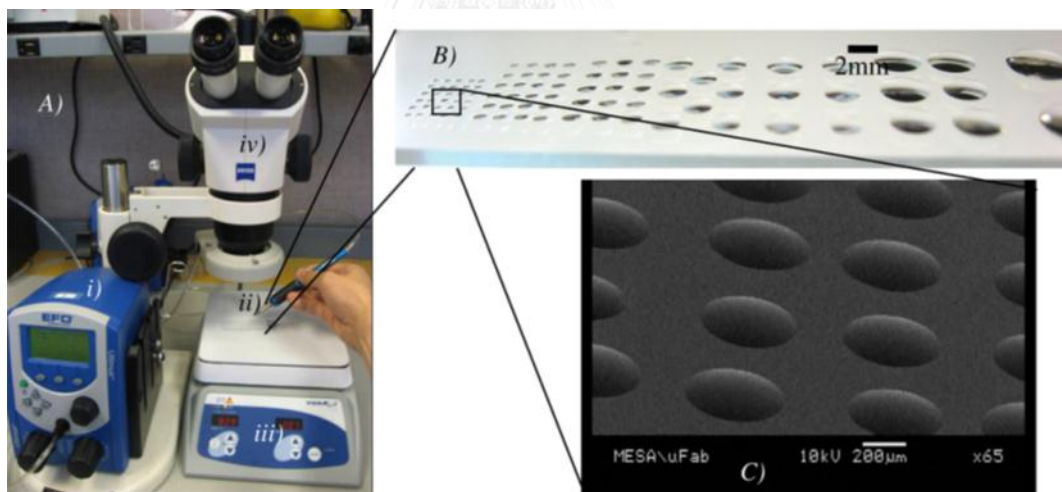


**Figure 2.6** Fabrication of ePDMS micro-lens array by moldless surface energy minimization technique [50].

### 2.2.3 The Thermal Reflow Process

Hsieh et al., 2011 [51] fabricated SU-8/ePDMS micro-lens array by the thermal reflow process. Firstly, the silicon wafer was spin coated on a layer of photoresist (PR) layer and the PR cylinders were patterned after photolithography. Then PR cylinder was heated at 150 °C for 40 s and formed micro-lens array with a spherical profile. The next step is spin-coating of IPDMS on the substrate. Then the IPDMS coated wafer was relaxed for 10 min to reduce roughness and cured at 80 °C for 90 min. After cooling to the room temperature, the PDMS mold can be easily detached from PR micro-lens wafer. After that the UV resin (SU-8) was dropped on the ePDMS mold and attached a cover glass on top the SU-8. Finally SU-8 layer was cured by UV light. The SU-8/ePDMS micro-lens array has long focal length with lens diameter in the range of 50-240  $\mu\text{m}$ .

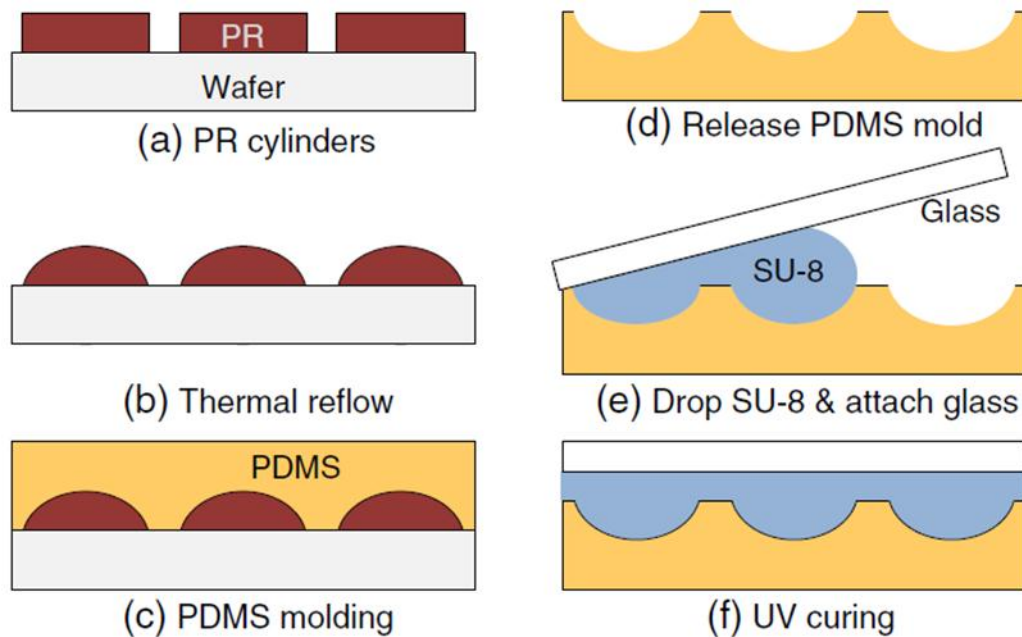


**Figure 2.7** Fabrication of ePDMS micro-lens array by thermal reflow process [51].

## 2.2.4 The Dielectrophoresis Force Technique

Wang et al., 2011 [52] fabricated ePDMS micro-lens arrays by dielectrophoresis force technique. The flexible printed circuit (FPC) is composed of concentric circular electrode array. A 100- $\mu\text{m}$  thickness of polyethylene (PE) membrane is attached onto FPC and coated by 20  $\mu\text{m}$  thickness of Teflon. A dropping of 0.35  $\mu\text{L}$  of IPDMS was dropped onto modified surface and cured at 90  $^{\circ}\text{C}$  for 30 min. Finally, the ePDMS micro-lens array is derived from the detaching of PE membrane from the FPC. The contact angle of IPDMS droplets can be controlled by the voltage diving circuit and gradient voltage applied on the FPC. The ePDMS micro-lens array has the contact angle of 25 $^{\circ}$ -60 $^{\circ}$  and radius of curvature of 0.45-1.80 mm. The dielectrophoresis force technique is appropriated for mass scale production of ePDMS micro-lens array.

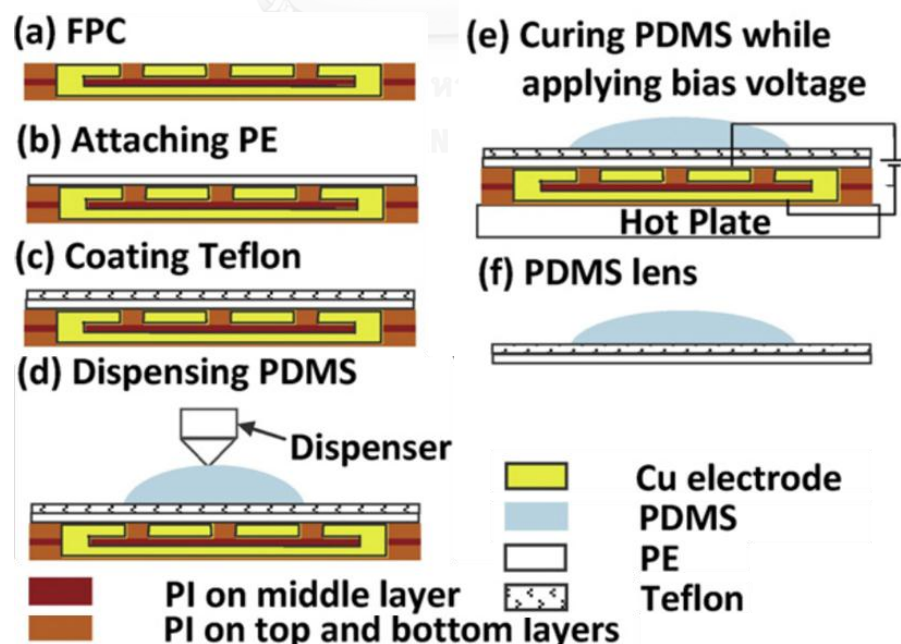


**Figure 2.8** Fabrication of ePDMS micro-lens array by the dielectrophoresis force technique [52].

### 2.2.5 The Hanging Droplet Technique

Lee et al., 2014 [37] developed a process for ePDMS lens fabrication by the hanging droplet technique. A  $\sim 100\text{-}\mu\text{l}$  IPDMS was dropped on the glass slide and cured at  $70\text{ }^\circ\text{C}$  for 15 min to form the first layer. For the second layer, IPDMS was dropped on ePDMS film from the first step and immediately inverted. Then it was cured at  $70\text{ }^\circ\text{C}$  for 15 min. The repetition of the third and fourth layer was performed with the same process as the second step. The hanging droplet technique can control the focal length in the range 1-15 mm by changed the layer number of IPDMS droplet.

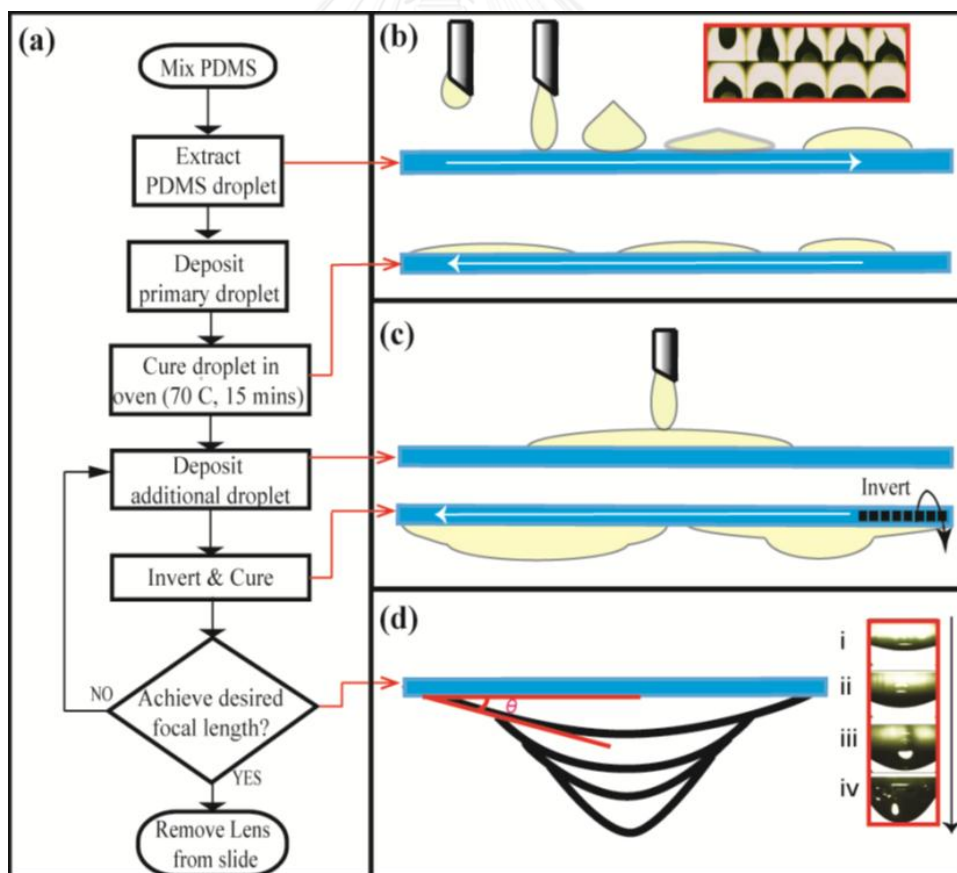


**Figure 2.9** Fabrication of ePDMS micro-lens array by the hanging droplet technique [37].

### 2.2.6 The Inkjet Printing Technique

Sung et al., 2015 [43] produced ePDMS lens by inkjet printing technique. A small volume of IPDMS in the range 10-200  $\mu\text{L}$  was injected onto controlled temperature preheated surface (60-200  $^{\circ}\text{C}$ ). The curvature and focal length can be controlled by IPDMS volume and temperature of preheated surface. This technique can fabricate plano-convex lens with a focal length as short as 5.6 mm, high-resolution as 1  $\mu\text{m}$ , and magnification as 100X. The ePDMS lens from this technique can observe the human skin and hair follicle.

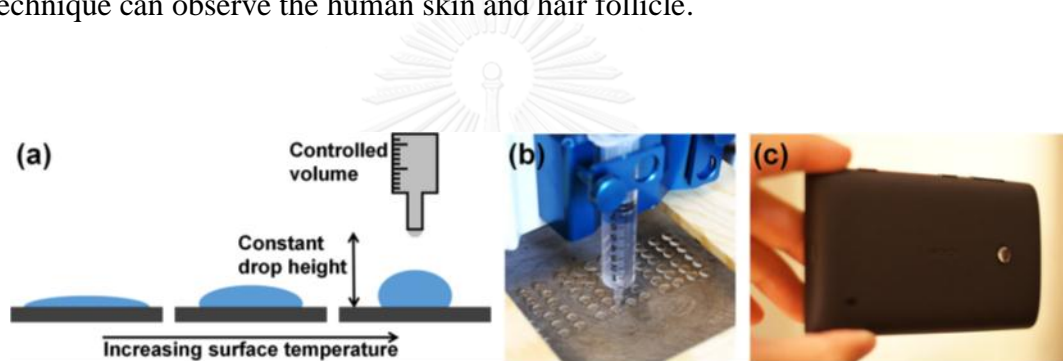


**Figure 2.10** Fabrication of ePDMS lens by inkjet printing technique.

The advantages and disadvantages of each fabrication technique are shown in Table 2.2.



**Table 2.2** Summary of the techniques for ePDMS lens fabrication

<b>Methods, author, and year</b>	<b>Advantages</b>	<b>Disadvantages</b>
Replica Molding Shih et al., 2006 [49]	- Good light focusing - Smooth surface	- Complicate process - Low reproducibility
Moldless Surface Energy Minimization Cruz-Campa et al., 2010 [50]	- Rapid fabrication - Precisely control of PDMS volume - Moldless method	- Require expensive instrument
Thermal Reflow Process Hsieh et al., 2011 [51]	- Controllable focal length - Good light focusing	- Complicated processing - Require photolithography instrument
Dielectrophoresis Force Wang et al., 2011 [52]	- Controllable contact angle - Mass-scale production	- Difficult to duplicate - Advanced and expensive instrument
Hanging Droplet Lee et al., 2014 [37]	- Moldless method - Smooth surface	- Multistep process - Air bubble in lenses - Low repeatability
Inkjet Printing Sung et al., 2015 [43]	- Rapid process - Moldless method - Smooth surface	- High temperature - Air bubble in lenses - Non reproducibility

## **CHAPTER III**

### **EXPERIMENTAL SECTION**

#### **3.1 CHEMICALS, MATERIALS, AND INSTRUMENTS**

- 3.1.1 Polydimethylsiloxane (Sylgard<sup>®</sup> 184, Dow Corning, USA)
- 3.1.2 Height adjustable stage
- 3.1.3 Small LED lamp
- 3.1.4 Chamois or cleaning fabrics
- 3.1.5 Plastic cup
- 3.1.6 Hotplate stirrer (Heidolph)
- 3.1.7 Syringe Pump (NE-1000 Programmable Single Syringe Pump, New Era Pump System, Inc., USA)
- 3.1.8 Smartphone (iPhone 6s Plus)
- 3.1.9 ChulaSmartLens with 20X magnification
- 3.1.10 Laser cutting machine (T-BROS LASER)
- 3.1.11 Optical Microscope, Carl Zeiss: Axio Scope.A1
- 3.1.12 Standard goniometer (Model 200-F1, Ramé-Hart Instrument Co., USA)

## 3.2 FABRICATION PROCEDURES OF ePDMS PLANO-CONVEX LENS

### 3.2.1 Preparation of PMMA Circular Disk

PMMA circular disks were prepared by cutting of 1 mm-thick poly(methylmethacrylate) (PMMA) sheet using laser cutting machine (T-BROS LASER) operating with cutting speed of 30 mm/s and laser power of 50%. The circular disks with various diameters (2.0, 3.0, 4.0, 5.0, 6.0, 7.0, 8.0, 9.0, and 10.0 mm) were prepared and subsequently employed as substrates for fabrication ePDMS plano-convex lenses with precisely controlled diameter. as shown in Figure 3.1.

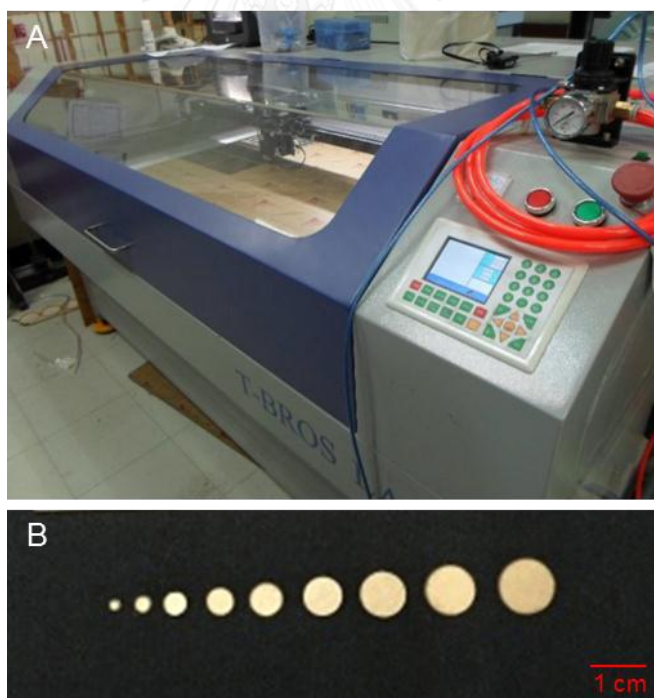


**Figure 3.1** Photographic images of (A) the laser cutting machine and (B) the PMMA circular disks (with diameter of 2.0, 3.0, 4.0, 5.0, 6.0, 7.0, 8.0, 9.0, and 10.0 mm) used in the fabrication of ePDMS plano-convex lenses.

### 3.2.2 Preparation of IPDMS

The IPDMS (Sylgard<sup>®</sup> 184, Dow Corning, USA) was prepared by mixing of the PDMS base and curing agent with the recommended weight ratio of 10:1 and stirred for 5 min, as shown in Figure 3.2. The homogenous IPDMS mixture was placed in vacuum chamber for 30 min in order to degasing and removing of residual solvent [53]. After that, the IPDMS was filled into a 10-mL syringe and kept in refrigerator. To precisely controlled the dispensed volume, a syringe pumped (NE-1000 Programmable Single Syringe Pump, New Era Pump System, Inc., USA) was used. The IPDMS was dropped onto a PMMA circular disk at ~10 mm above the circular disk in order to avoiding an impact-induced spreading of the falling droplet. The IPDMS was left undisturbed for at least 5 min to allow the droplet to transform into a stable spherical cap before a thermal curing at 80 °C for 30 min. The ePDMS plano-convex lenses with reproducible curvature, focal length, imaging area, field of view, and magnification could be fabricated.

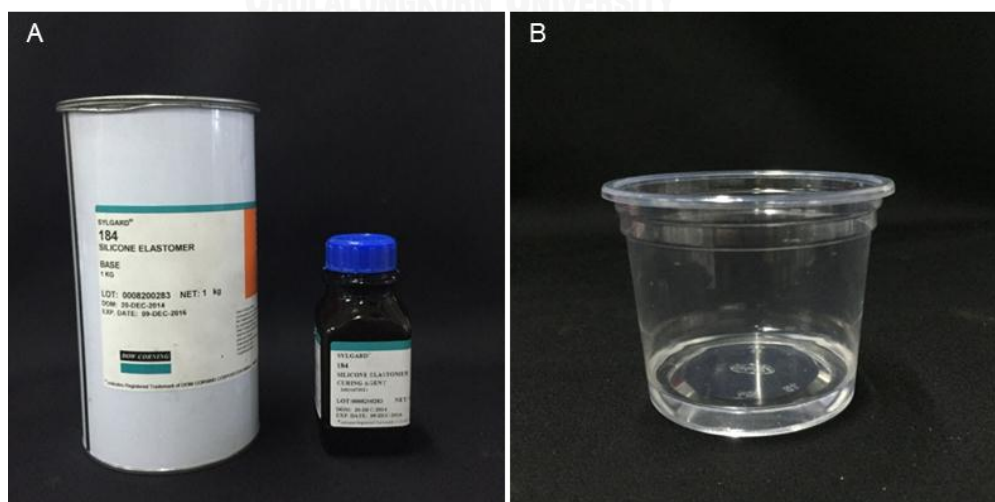


**Figure 3.2** Photographic images of (A) Sylgard<sup>®</sup> 184 and (B) the mixed IPDMS for ePDMS lens fabrication.

### **3.3 EFFECT OF EXPERIMENTAL PARAMETERS ON THE FABRICATION OF ePDMS PLANO-CONVEX LENS**

#### **3.3.1 Effect of Circular Disk Material on IPDMS Spreading**

The flat surface of PMMA sheet, PDMS film, polycarbonate (PC) sheet, and glass was employed as substrates for ePDMS plano-convex lens fabrication. A 15- $\mu$ L of IPDMS from 3.2.2 was dropped on the flat surface by syringe-pump at ~10 mm above the surfaces in order to avoiding an impact-induced spreading of the falling droplet. The spreading of IPDMS on various surfaces was monitored by video recording with iPhone 6s Plus.

#### **3.3.2 Effects of Drop Position**

The PMMA circular disk was put on the substrate at the desired height. Then, a 15- $\mu$ L of IPDMS from 3.2.2 was dropped onto 3 mm PMMA circular disks by syringe pump at ~10 mm above the flat surfaces in order to avoiding an impact-induced spreading of the falling droplet. Then, the IPDMS droplets were dispensed at 0 mm, 0.5 mm, and 1 mm from the center of the disk. The IPDMS axisymmetrically spread over the circular disk. After that the IPDMS was left undisturbed for at least 5 min to allow the droplet transforming into a stable spherical cap structure before thermally cured at 80 °C for 30 min. The spreading and hemispherical forming of IPDMS was monitored by video recording with iPhone 6s Plus.

### 3.3.3 Effects of Curing Temperature

The PMMA circular disk was put on a substrate. A 40- $\mu\text{L}$  of IPDMS was dropped onto the 6 mm PMMA circular disk at  $\sim 10$  mm above the flat surfaces in order to avoid an impact-induced spreading of the falling droplet. The IPDMS was left undisturbed for at least 5 minutes to allow the droplet transforming into a stable spherical cap structure before thermally cured at room temperature 80 °C, 100 °C, 150 °C, and 200 °C. The process was monitored by video recording with iPhone 6s Plus.

### 3.3.4 Effects of IPDMS Volume

To demonstrate a capability for fabricating lenses of the same diameters with different focal lengths, a series of 6-mm lenses was fabricated using various volumes of IPDMS. The first PMMA circular disk was put on a substrate at the desired height. Then, the ePDMS plano-convex lenses were prepared by dispensing of various IPDMS volumes (5  $\mu\text{L}$ , 10  $\mu\text{L}$ , 15  $\mu\text{L}$ , 20  $\mu\text{L}$ , 25  $\mu\text{L}$ , 30  $\mu\text{L}$ , 35  $\mu\text{L}$ , and 40  $\mu\text{L}$ ) onto the PMMA circular disk before thermally cured at 80 °C for 30 min. The microscope images were captured by using ePDMS plano-convex lens attached iPhone 6s Plus.

### 3.3.5 Effects of Circular Disk Diameters

To demonstrate a capability for fabricating lenses of certain diameter with different focal length, a series of lenses was fabricated using various diameters of PMMA circular disk. The first PMMA circular disk was put on the substrate. The plano-convex lens was prepared by dispensing various diameters of substrate and

various volume of IPDMS (2 mm (3  $\mu$ L), 3 mm (6  $\mu$ L), 4 mm (15  $\mu$ L), 5 mm (30  $\mu$ L), 6 mm (40  $\mu$ L), 7 mm (60  $\mu$ L), 8 mm (70  $\mu$ L), 9 mm (90  $\mu$ L), and 10 mm (100  $\mu$ L)). The specified volumes are the highest possible volumes of IPDMS that can be dispensed onto the corresponding PMMA disks before thermally cured at 80 °C for 30 min. The microscope images were captured by using ePDMS plano-convex lens attached iPhone 6s Plus.

### **3.3.6 Effects of Circular PDMS Thickness**

To manipulate the magnification and utility of the ePDMS plano-convex lens, a 6-mm (40  $\mu$ L) lens was fabricated with various thickness of PDMS film. The lens (6 mm, 40  $\mu$ L) was attached on top of a 6-mm PDMS disk using 5- $\mu$ L IPDMS as a binder. The IPDMS binder was solidified by heating on a hotplate at 150 °C for 1 min. The thickness of the PDMS disk was adjusted (1, 2, 3, and 4 mm) in order to manipulating the focal length. The microscope images were captured by using ePDMS plano-convex lens attached iPhone 6s Plus.

### **3.3.7 Applications of ePDMS Plano-Convex Lens**

The fabricated ePDMS plano-convex lens attached on iPhone 6s Plus camera were used for capturing the microscopic image. The microscopic images of samples including new USD100 banknote, Chulalongkorn University logo, gunshot residues (GSRs) generated by a point-blank shooting on a cotton fabric, and bullets were acquired and compared.

### 3.4 CHARACTERIZATIONS

The determination of the focal length, magnification, and viewing area of the lenses are shown as follows:

#### 3.4.1 Contact Angle

The contact angle of the ePDMS plano-convex lens was measured using the photographic capability of a standard goniometer (Model 200-FI, Ramé-Hart Instrument Co., USA.). The instrument used for measuring the contact angle is shown in Figure 3.3.



**Figure 3.3** Photographic image of the contact angle measurement.



### 3.4.2 Focal Length

In this work, the focal length is defined as the shortest distance between the object and the curved surface of the lens. The distance with the most intense laser spot was recorded as the focal length, as shown in Figure 3.4.

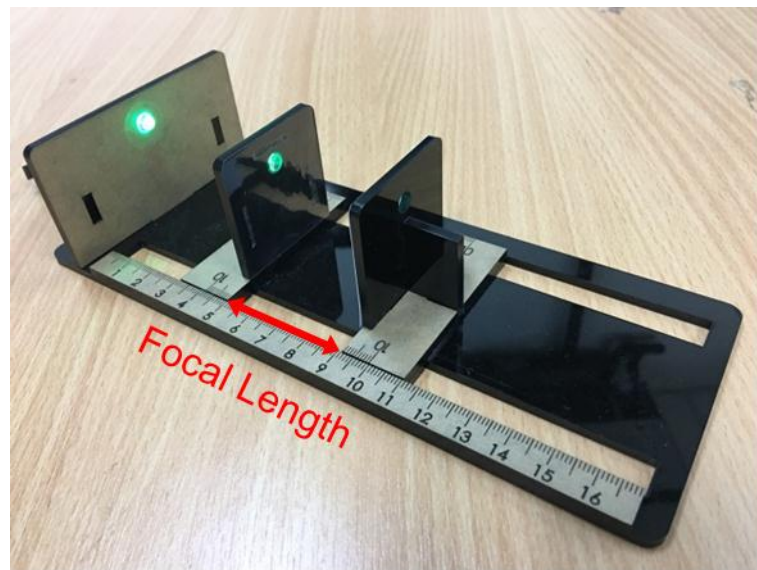


**Figure 3.4** Photographic image of the focal length measurement

### 3.4.3 Magnification

The magnifications of the lenses are calculated by Equation 1 [35, 54]

$$M = 250/f \quad (1)$$

where M: magnification and

f: focal length

### 3.4.4 Viewing Area

The viewing areas are measured by capturing of the 1-mm square grid paper with iPhone 6s Plus coupled with ePDMS plano-convex lens. The viewing areas were measured directly from the microscopic images using ImageJ program (ImageJ is a public domain, Java-based image processing program developed at the National Institutes of Health, USA).

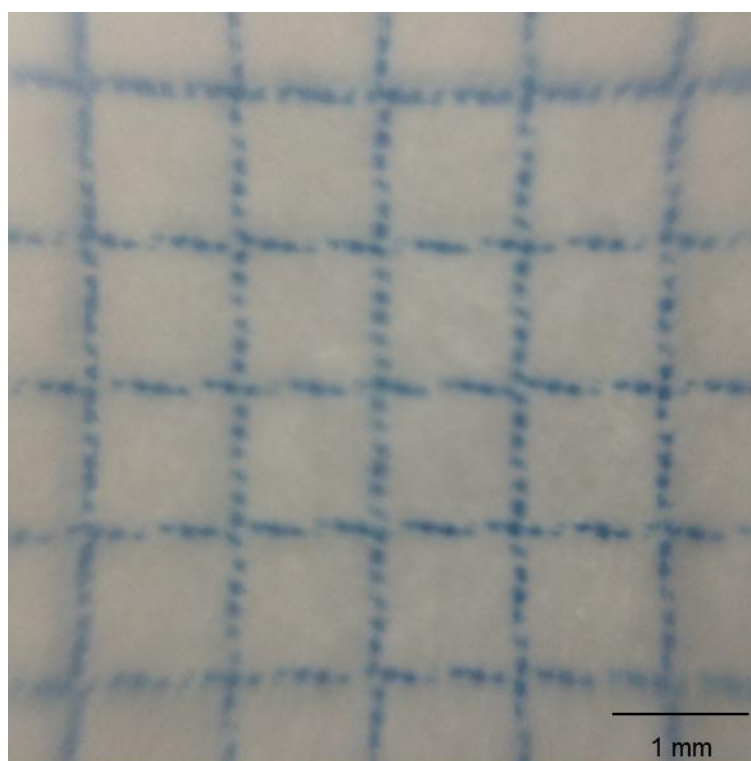


**Figure 3.5** Photographic image of 1-mm square grid paper for viewing area measurement.

## **CHAPTER IV**

### **RESULTS AND DISCUSSION**

#### **4.1 PRELIMINARY OBSERVATIONS**

The idea of development on employing ePDMS for fabricating plano-convex lens by the various methods was firstly reported in the publication by Shih et al. in 2006. The ePDMS lenses were fabricated by various technique including replica molding [49], moldless surface energy [50], thermal reflow process [51], filling circular holes [55], hanging drop [37], and inkjet printing [43]. These have several drawbacks including air-bubble when using high temperature in curing lens, rough surface when using old mold, and the requirement of complex methods and expensive instruments. To solve those problems, this research developed the new technique for fabrication of plano-convex lens by using the confined sessile drop technique. The confined sessile drop technique takes advantage of the resistance to spreading by sharp edge for control the size and shape of lenses. We can couple the ePDMS plano-convex lens with the smartphone camera and transform the device to portable smartphone digital microscope. Applications of portable smartphone digital portable microscope for imaging such as micro-print of banknote, animal and biotic components, medical diagnostic, and gun shoot residue were demonstrated.

## 4.2 FABRICATION AND TESTING OF ePDMS PLANO-CONVEX LENSES

To explore the potential of the confined sessile drop technique for ePDMS plano-convex lens fabrication, we investigated the spreading of IPDMS droplet on flat surfaces of poly(methyl methacrylate) (PMMA) sheet, PDMS film, polycarbonate (PC) sheet, and glass slide (Figure 1). As the 15- $\mu$ L IPDMS droplets reached the surfaces, it spread axisymmetrically in a stick-slip manner under the influence of gravitational force while the interfacial tension force made the surface of the IPDMS atomically smooth [55]. The IPDMS droplet transformed into a hemispherical cap within 1 s and a large spherical cap of low curvature within 5 s. At 10 s, the 15- $\mu$ L IPDMS droplets reached spreading diameters of 5.6 mm on PMMA sheet, 5.1 mm on PDMS film, 5.3 mm on PC sheet, and 5.8 mm on glass slide. The contact angle decreased from 105° to 31° (glass), 112° to 32° (PMMA), 108° to 28° (PC), 128° to 49° (PDMS). The spreading continued and the droplet transformed into a thin film with zero contact angle in 30 min (data not shown). The IPDMS spread faster on the solid surfaces in the order glass > PMMA > PC > PDMS because glass and IPDMS have much different interfacial tension so IPDMS is the fastest flow on the glass.

Water droplet with high interfacial tension (72.8 dyne/cm) retains its hemispherical shape on polymeric surfaces with certain contact angle governed by Young's law. The IPDMS with low interfacial tension (20-23 dyne/cm), on the other hand, spread into a thin film with equilibrium (thermodynamic) contact angle of 0° [56-57]. However, within a few seconds after discharging from syringe, one can cure the IPDMS into a working ePDMS plano-convex lens as the droplet attains an optimal curvature with near 90° contact angle. By thermally cure the sessile drop within 2 s

(i.e., by dispensing the droplet on to a pre-heated substrate), the solidified PDMS spherical cap become a plano-convex lens as the PDMS elastomer is transparent in the UV/visible region with a refractive index of  $\sim 1.42$  [56]. However, due to high viscosity and temperature-dependent curing rate of IPDMS, a rapid curing at 180-200 °C makes the fabrication of PDMS elastomeric lenses with reproducible curvature, focal length, and diameter impossible. The viscosity of the liquid PDMS increases rapidly within a short storage period, especially at high temperature and high concentration of hardener [58]. Air bubbles always developed within the PDMS elastomeric lens when curing at temperature greater than 80 °C (Figure 4.2). A production loss due to irregular curvatures and air bubbles is common under a high temperature curing. As a result, PDMS micro-lenses and PDMS milli-lens were normally fabricated by controllable approaches such as lithography, thermal-reflow process, or hanging drop technique [37, 50, 59]. However, those techniques require a complex instrument or multi-step production protocol.

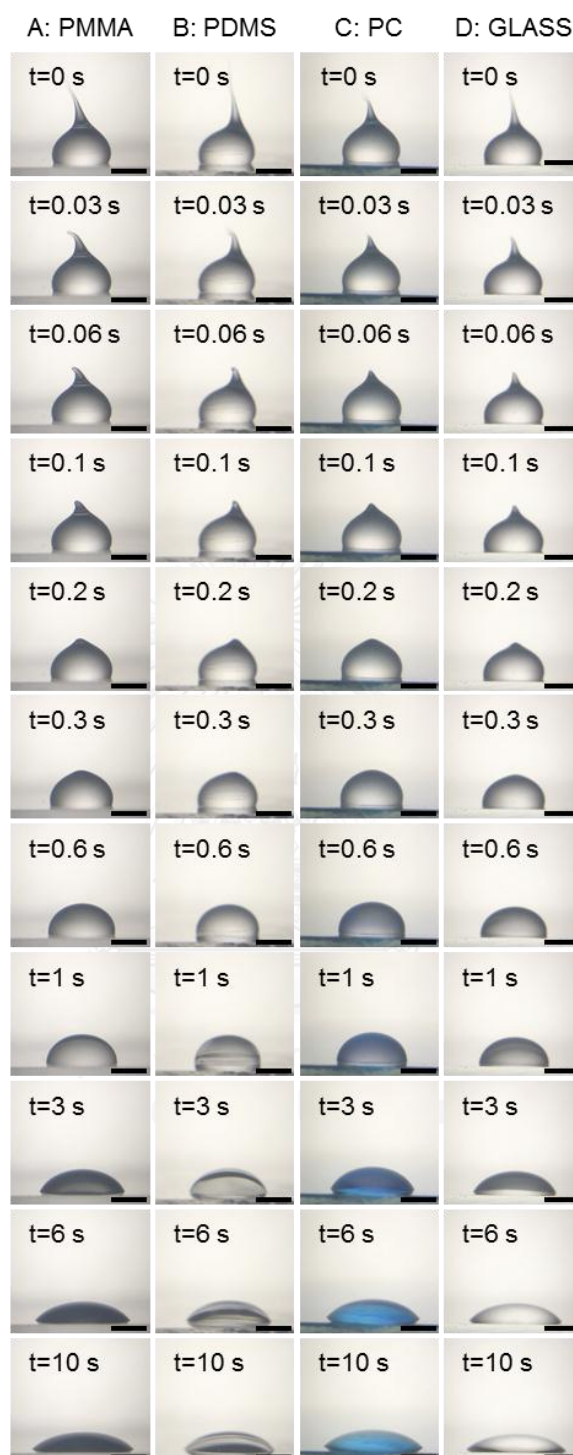


**Figure 4.1** Time-dependent photographic images of 15- $\mu$ L IPDMS sessile drops axisymmetrically spread on selected flat surfaces of (A) PMMA sheet, (B) PDMS film, (C) PC sheet, and (D) glass slide. Scale bars indicate 2 mm.

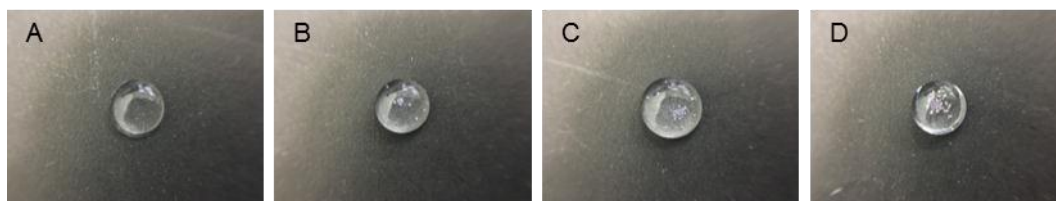


**Figure 4.2** Photographic image of (A) a bubble-free ePDMS plano-convex lens prepared by the confined sessile drop technique by curing a spherical cap IPDMS on 5-mm PMMA circular disk at 80 °C for 30 min. The ePDMS lens with air bubbles prepared by dispensing a droplet of IPDMS onto a pre-heated (B) 100 °C, (C) 150 °C, and (D) 150 °C glass slide.

To fabricate the ePDMS plano-convex lenses with a more efficient, controllable, and reproducible manner, we developed the confined sessile drop technique that takes advantage of the resistance to spreading by sharp edge for reproducibly fabricating spherical cap of IPDMS on a circular PMMA disk. A commercially available 1-mm thick PMMA sheet with flat surfaces was laser cut into a disk (2-10 mm in diameter) and was employed as a substrate for reproducibly making lens with controllable size and focal length. As the IPDMS droplet touched a PMMA disk, it axisymmetrically spread over the entire 3-mm PMMA disk within 2 s (Figures 4.3A and 4.4). The three phase contact line (IPDMS/Air/PMMA) radially expanded with a concomitant decreasing of contact angle. When the IPDMS reached the edge of the PMMA disk, the spreading stop with a local contact angle of  $\theta_p$ . Unlike those in Figure 4.1A where the IPDMS keep spreading and eventually become a thin film, the spherical cap in Figure 4.3 was stabilized without flowing over the subtended edge. The IPDMS spherical caps were highly stable as the curvature was

retained without an observable change for at least 24 h. The liquid PDMS does not flow across the sharp edge of the disk as long as  $\theta_p$  is smaller than the critical contact angle for spreading over the edge ( $\theta_c$ ) defined by the Gibbs inequality equation as:[57-58, 60-61]

$$\theta_c = (180 - \phi) + \theta_e \quad (2)$$

Where  $\phi$  is the subtended angle at the edge (in this case  $\phi = 90^\circ$ ),  $\theta_e$  is the equilibrium (thermodynamic) contact angle (in this case  $\theta_e = 0^\circ$ ) [57, 60]. From our experiment, the IPDMS spread into a thin film ( $\theta_e = 0^\circ$ ) on PMMA sheet within 30 min. According to Eq. 1,  $\theta_c$  in our system equals  $90^\circ$ .

A unique advantage of the confined sessile drop technique was realized as we could fabricate exact same spherical caps even though the droplets were deposited off-center of the PMMA disks (Figures 4.3B and 4.3C). The edge effect prevent the viscous liquid to flow down the subtended corner while the interfacial tension force pulled the IPDMS to the center and form into a spherical cap within 6 s. The IPDMS spherical caps can be thermally cured (80 °C, 30 min) into ePDMS plano-convex lenses. The 3-mm ePDMS plano-convex lenses in Figures 4.3A-4.3C has focal length of 5.0 mm with magnification of ~50X and viewing area of 5.0x3.8 mm<sup>2</sup>. The magnification power is calculated according to the expression: Magnification  $X=250/f$ , where  $f$  is the focal length in mm [35, 54]. Figs. 4.4B-D show images of micro-printing on a new USD100 banknote (series 2009 A) acquired by an iPhone 6s Plus equipped with the fabricated lenses. Details and textures of the micro-printing



could be clearly imaged. Moreover, by taking advantages of the digital zoom capabilities, images with a higher magnification ( $\sim 200\times$ ) could be acquired (Figure 4.4E-G). The high pixel density photographic capability of smartphones enables a microscopic imaging without a limitation of electrical power supply [62].



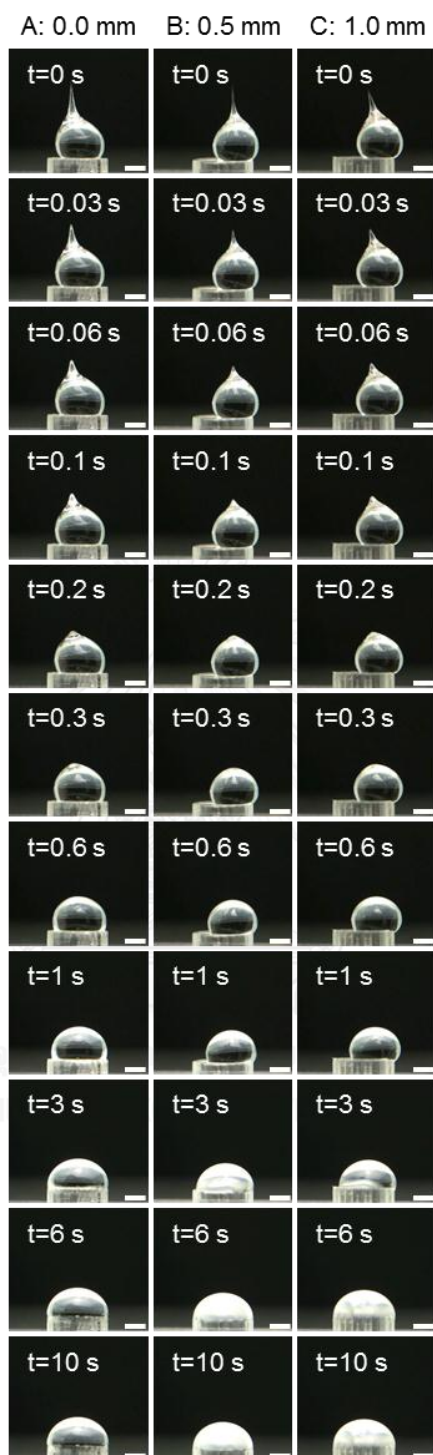


**Figure 4.3** Time-dependent images of 15- $\mu$ L IPDMS confined sessile drops spreading on 3-mm PMMA. The droplets were deposited at (A) 0.0, (B) 0.5, and (C) 1.0 mm from the center of the disk. Scale bars indicate 1 mm (A-C)

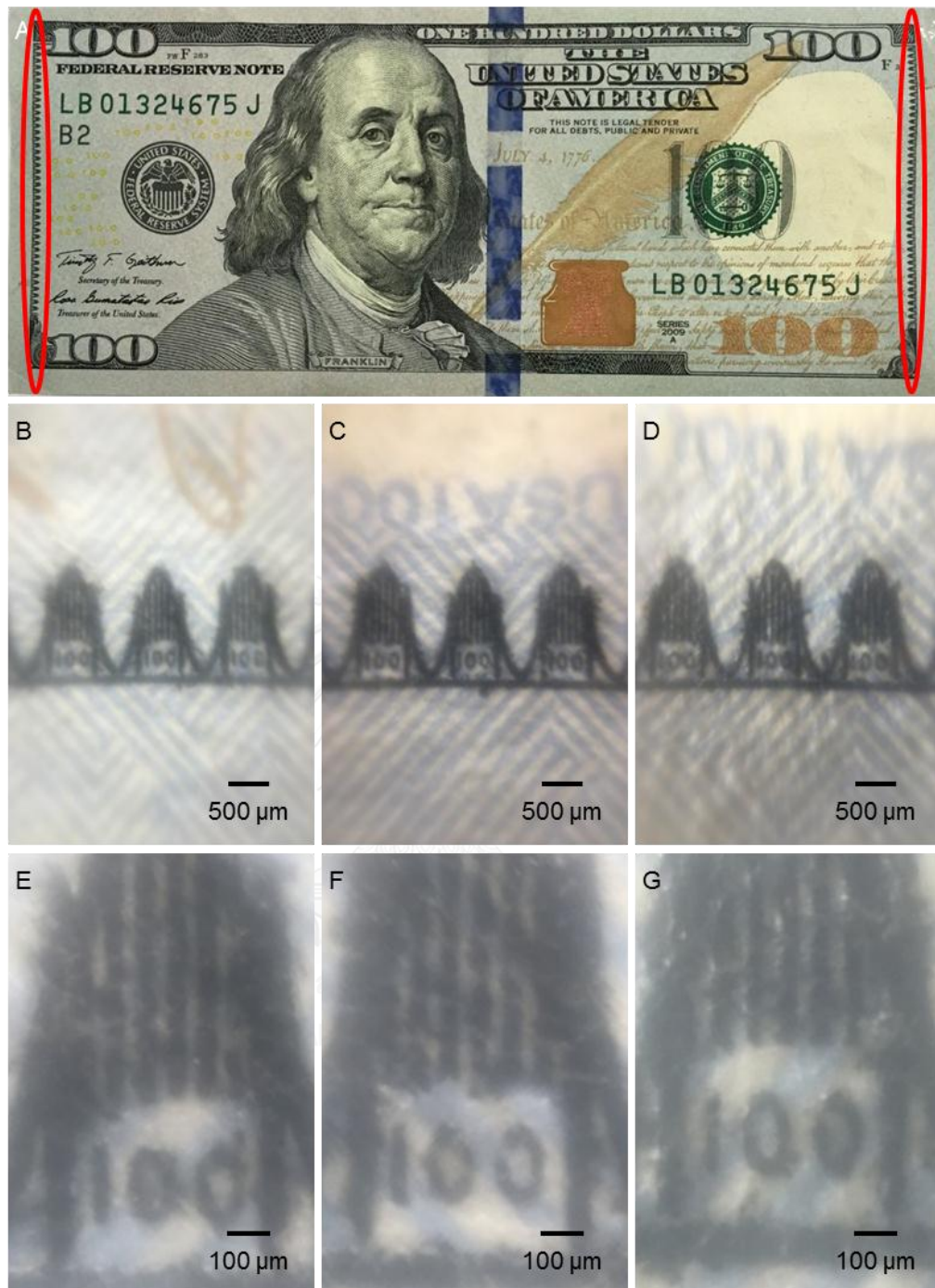


**Figure 4.4** The front side of a new USD 100 banknote show in (A). The red circles indicate arrays of micro-printings. (B-D) show the microscopic images of micro-printing acquired with 3-mm ePDMS plano-convex lenses. (E-G) are the corresponding images with 4X digital zoom. Scale bars indicate 500  $\mu\text{m}$  (B-D), and 100  $\mu\text{m}$  (E-G).

To demonstrate efficiency, reproducibility, and controllability of the confined sessile drop technique, we produced 6-mm ePDMS plano-convex lenses of various focal lengths by dispensing different volumes of IPDMS onto 6-mm PMMA disks. As shown in Figure 4.5 and 4.6, a larger dispensed volume produced lens with a shorter focal length. The focal length decreased from 34.2 mm to 13.0 mm while the contact angle increased from  $22^\circ$  to  $95^\circ$  as the dispensed volume was increased from 5  $\mu\text{L}$  to 40  $\mu\text{L}$  (Figure 4.5 and 4.6). The narrow distributions of the focal length implied a high degree of reproducibility of the fabrication technique. Due to the non-volatile and dimensional stability nature of the IPDMS, the contact angles of the spherical caps equaled those of the lenses. The contact angle of ePDMS plano-convex lens in Figure 4.5 and 4.6 agree with the Gibbs inequality condition as  $\theta_p$  increased from  $22^\circ$  to  $95^\circ$  when the dispensing volumes were increased from 5  $\mu\text{L}$  to 40  $\mu\text{L}$ . However, at a dispensing volume of 45  $\mu\text{L}$ ,  $\theta_p$  is much greater than  $90^\circ$  and the IPDMS flow over the edge (Figure 4.7). The confined sessile drop of IPDMS was highly stable and self-cured into ePDMS plano-convex lens in 24 h at room temperature ( $30^\circ\text{C}$ ). It is possible to make PDMS elastomeric lens with contact angle slightly greater than  $90^\circ$  by curing the IPDMS spherical cap before it flows over the edge (Figure 4.6H). The detailed printing of Benjamin Franklin's eyes on the front side of a new USD100 banknote could be clearly imaged with a smartphone digital microscope (iPhone 6s Plus) equipped with the fabricated ePDMS plano-convex lenses (Figures 4.6A-H).

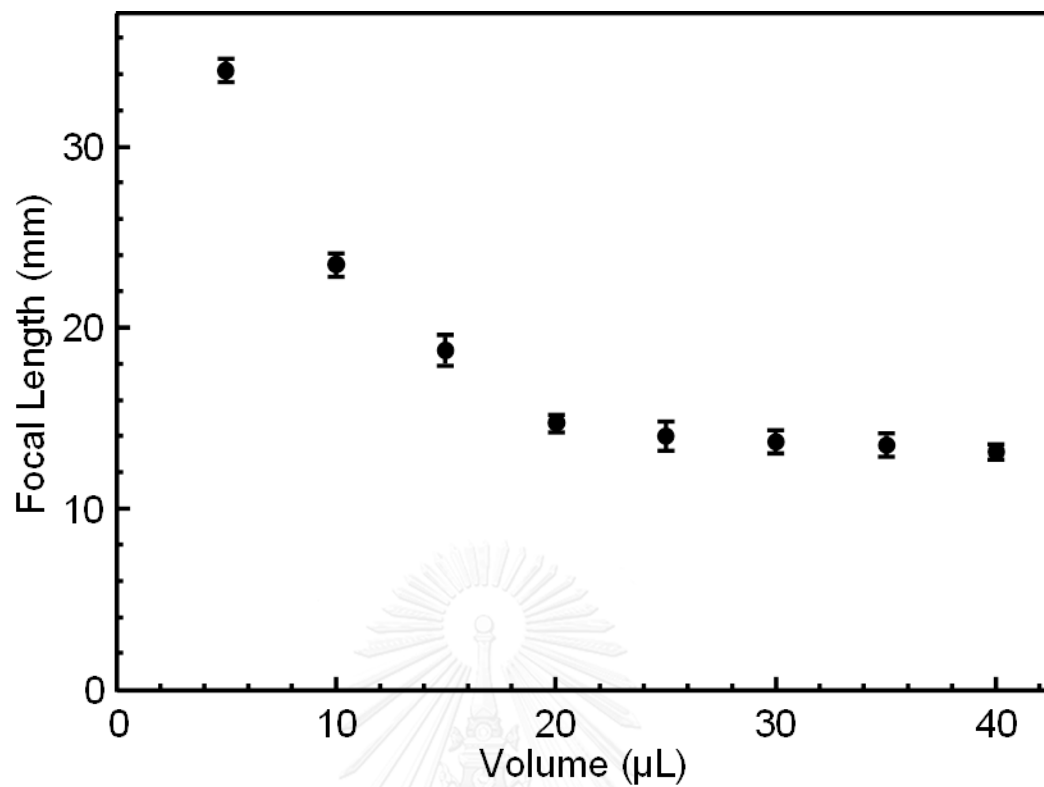


**Figure 4.5** 6-mm ePDMS plano-convex lens of various focal lengths fabricated by dispensing 5, 10, 15, 20, 25, 30, 35, and 40  $\mu\text{L}$  IPDMS on 6-mm PMMA disks. The standard deviation (SD) bar of each lens set was calculated from 20 lenses.



**Figure 4.6** Microscopic images of the Benjamin Franklin's eyes on the front side of a new USD100 banknote were taken by an iPhone 6s Plus coupled with the 6-mm ePDMS plano-convex lens of various focal lengths fabricated by dispensing (A) 5  $\mu\text{L}$ , (B) 10  $\mu\text{L}$ , (C) 15  $\mu\text{L}$ , (D) 20  $\mu\text{L}$ , (E) 25  $\mu\text{L}$ , (F) 30  $\mu\text{L}$ , (G) 35  $\mu\text{L}$ , and (H) 40  $\mu\text{L}$  IPDMS. The viewing area (VA, 4:3 format) and contact angle (CA) were indicated in the images.

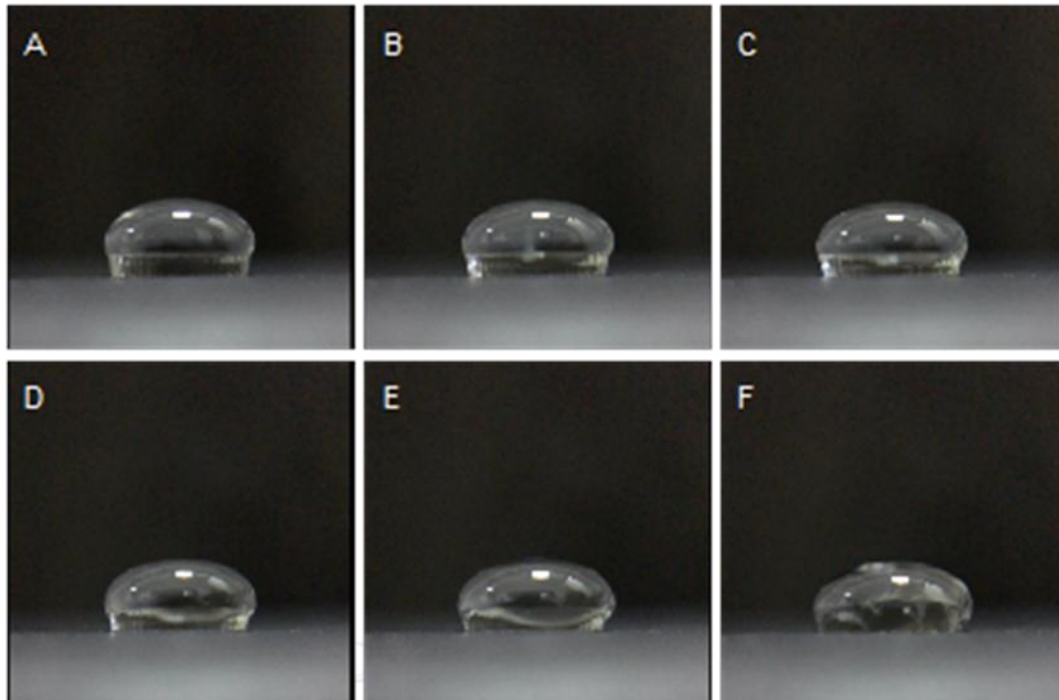


**Figure 4.7** Overflow of 45- $\mu$ L IPDMS on a 6-mm PMMA disk. The disk cannot hold the droplet as the local contact angle ( $\theta_P$ ) was much greater than the critical angle for spreading over the edge ( $\theta_C$ ) defined by the Gibbs inequality condition. In this case  $\theta_C=90^\circ$ .

The focal length of the ePDMS plano-convex lens could be controlled by using PMMA disk of different diameters (i.e., 2-10 mm disk with 1 mm increment). The maximum possible volume of IPDMS was dispensed on PMMA disk in order to fabricate a lens with the shortest focal length. The focal length decrease as the diameter of the disk becomes shorter. The focal length of the ePDMS plano-convex lens decrease from 55.2 mm to 3.4 mm as lens diameter was decreased from 10 to 2 mm (Figure 4.8 and 4.9). The narrow distributions of the focal length confirmed a high degree of reproducibility of the fabrication technique. The detailed microscopic

images of George Washington's statue at the rear of Philadelphia's Independence Hall on the flip side of a new USD100 banknote can be acquired.

By changing the volume of the dispensed IPDMS and diameter of the PMMA disk, we could systematically manipulate size, focal length, and magnification of the ePDMS plano-convex lens. A confined sessile drop on a smaller disk produces ePDMS plano-convex lens with higher curvature, shorter focal length, and higher magnification. The lenses can be efficiently fabricated with controllable and reproducible manner. Three sets of independent ePDMS elastomeric lenses with narrow distribution of contact angle and curvature confirm the reproducibility of the developed technique (Figure 4.10). Moreover, several sets of 100 5-mm lenses were fabricated and distributed for educational purpose (Figure 4.11). The ePDMS plano-convex lenses can be rapidly fabricated with a relatively low cost due to a small production lost. The material cost for making an ePDMS plano-convex lens shown in Figure 4.6H was ~0.01 USD (i.e., the cost included 10% material lost). Note: a 1.1 kg Kit Sylgard<sup>®</sup> 184 was offered by a local vendor at 260 USD. The total cost for making an ePDMS plano-convex lens is approximately 0.10 USD (i.e., the cost included liquid PDMS, PMMA sheet, electricity, and labor).



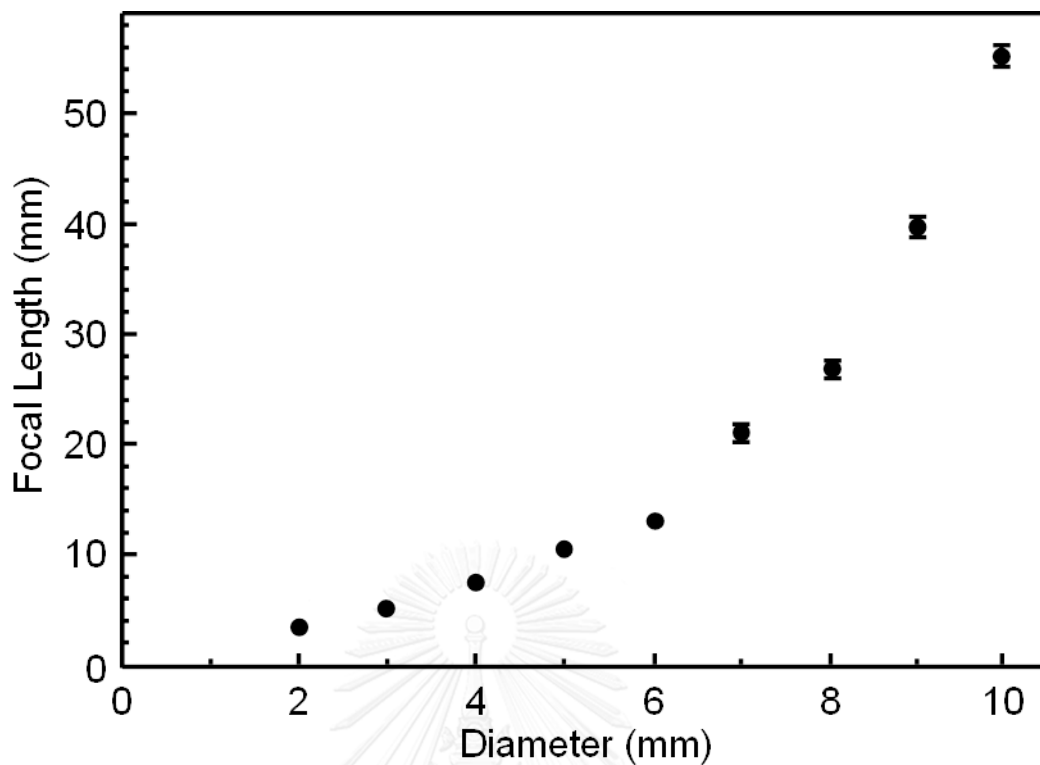


**Figure 4.8** The ePDMS plano-convex lenses of various focal lengths fabricated by dispensing the highest possible volume of IPDMS on PMMA disks: 2 mm (4  $\mu\text{L}$ ), 3 mm (6  $\mu\text{L}$ ), 4 mm (15  $\mu\text{L}$ ), 5 mm (30  $\mu\text{L}$ ), 6 mm (40  $\mu\text{L}$ ), 7 mm (55  $\mu\text{L}$ ), 8 mm (65  $\mu\text{L}$ ), 9 mm (80  $\mu\text{L}$ ), and 10 mm (100  $\mu\text{L}$ ). The SD bar of each lens set was calculated from 20 lenses.

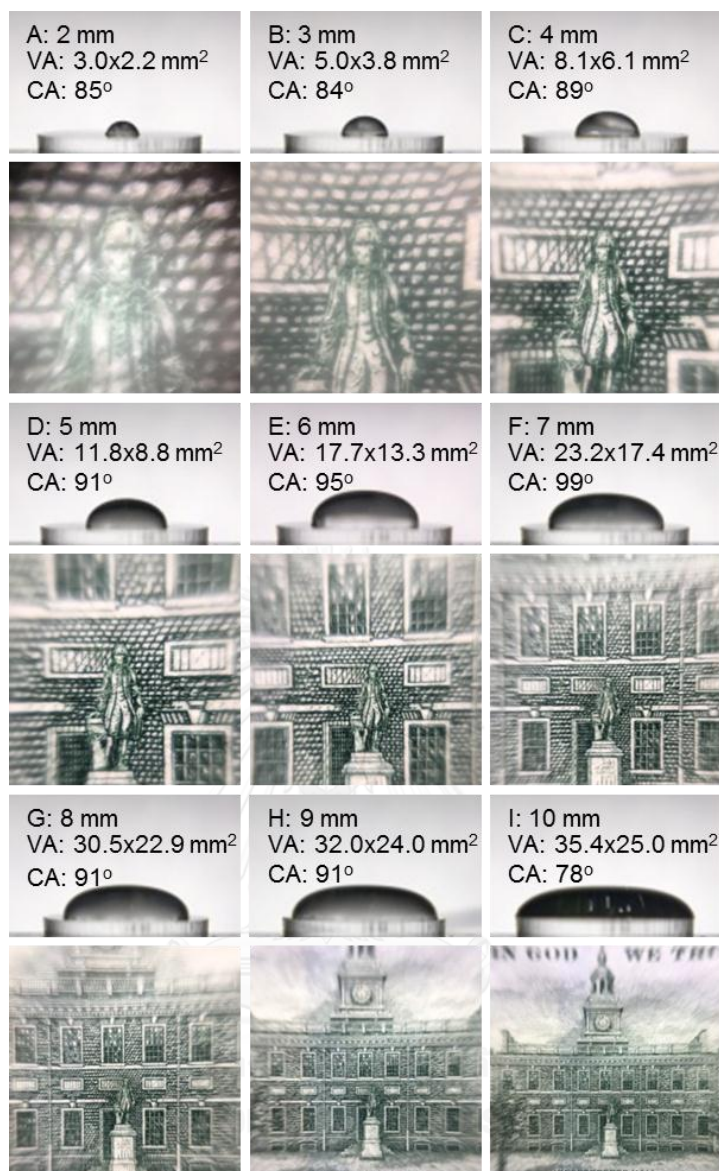


**Figure 4.9** Microscopic images of George Washington's statue on the flip side of a new USD100 banknote were taken by an iPhone 6s Plus coupled with the ePDMS plano-convex lenses fabricated by dispensing the highest possible volume of IPDMS on PMMA disks: (A) 2 mm (4  $\mu$ L), (B) 3 mm (6  $\mu$ L), (C) 4 mm (15  $\mu$ L), (D) 5 mm (30  $\mu$ L), (E) 6 mm (40  $\mu$ L), (F) 7 mm (55  $\mu$ L), (G) 8 mm (65  $\mu$ L), (H) 9 mm (80  $\mu$ L), and (I) 10 mm (100  $\mu$ L). The viewing area (VA, 4:3 format) and the contact angle (CA) were indicated.

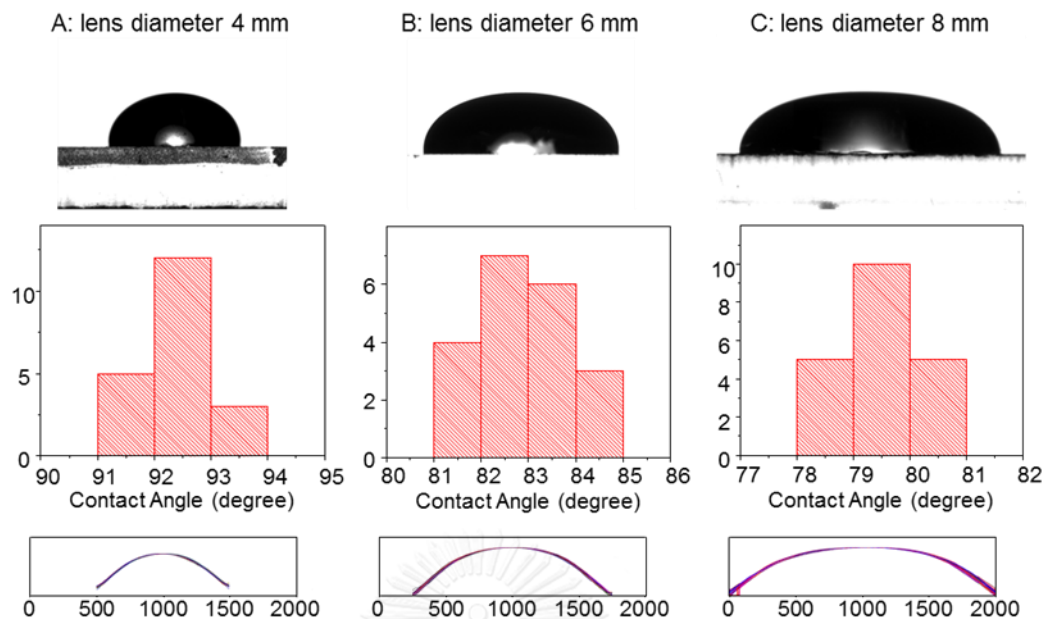


**Figure 4.10** Contact angles and curvatures of ePDMS plano-convex lens with diameter of (A) 4 mm, (B) 6 mm, and (C) 8 mm. The contact angles were measured from the images taken by the photographic capability of a standard goniometer (Model 200-F1, Ramé-Hart Instrument Co., USA). The lens curvatures were extracted from the contrast of the images by a MATLAB program. A set of 20 lenses was employed for each diameter. The narrow distributions indicate the reproducibility of the fabrication method.

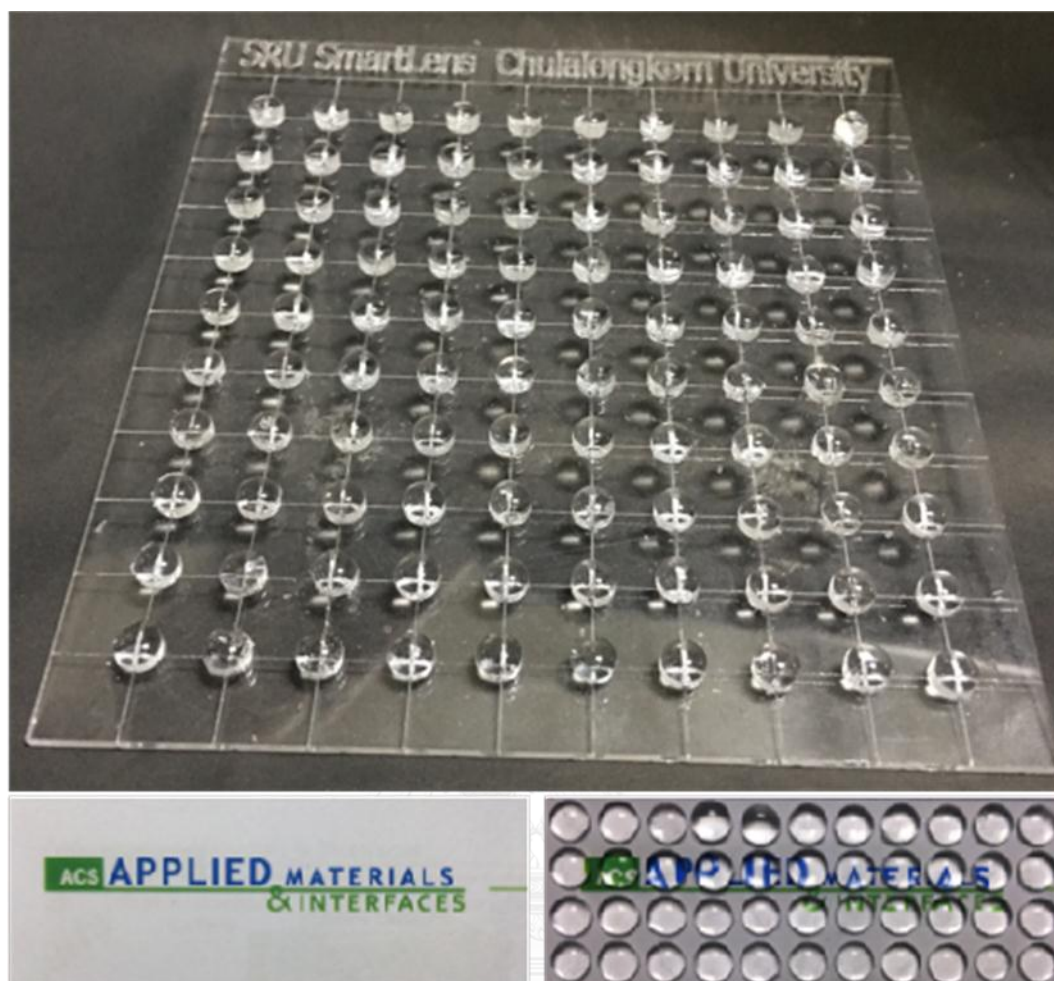


**Figure 4.11** A set of 100 ePDMS plano-convex lenses (5-mm diameter) fabricated by the confined sessile drop technique and their optical effect when placed on printed characters.

The ePDMS plano-convex lens detached from the PMMA disk can be re-attached onto the protecting window of a smartphone camera. However, lens with short diameter (i.e., 2-4 mm) is difficult to handle and easily fall off. One approach to make ePDMS plano-convex lens easily handle while improving surface adhesion is to fabricate lens with base [56, 63-64]. PDMS lens with base was directly fabricated on a PDMS film via an up-right approach [56], the hanging drop approach [37], and the

mold replication technique [63-64]. To simplify the fabrication process while achieving controllability and reproducibility, we developed the lens-on-base fusing technique. A newly fabricated ePDMS plano-convex lens was glued onto a PDMS disk of desired thickness and diameter by IPDMS (~5  $\mu$ L). After a thermal curing at 150 °C for 1 min, the ePDMS lens and PDMS base fused into a single PDMS lens with base. The fused layer was transparent without air bubbles. The radius of curvature  $R$  of a plano-convex lens (Figure 4.12) is defined by the radius of a circle with the longest arch superimposed on the envelop of the lens [65-69]. The 6-mm lens fabricated from 40- $\mu$ L IPDMS has a radius of curvature  $R$  of 4.0 mm and a focal length of 13.0 mm. The transparent PDMS base slightly increased the focal length of the lens from 13.0 mm (without PDMS base) to 15.0 mm (with 3-mm PDMS base). However, the focal length slightly decreased to 12.9 mm when a 4-mm thick PDMS base was employed. A thicker base is not recommended as it makes the lens too heavy and rigid. A large PDMS base is particularly beneficial for small lens as it increases the contact area while improving adhesion of lens with the flat surface of camera window. The PDMS base prevents lens damage and tearing during handling but insignificantly affected the focal length.

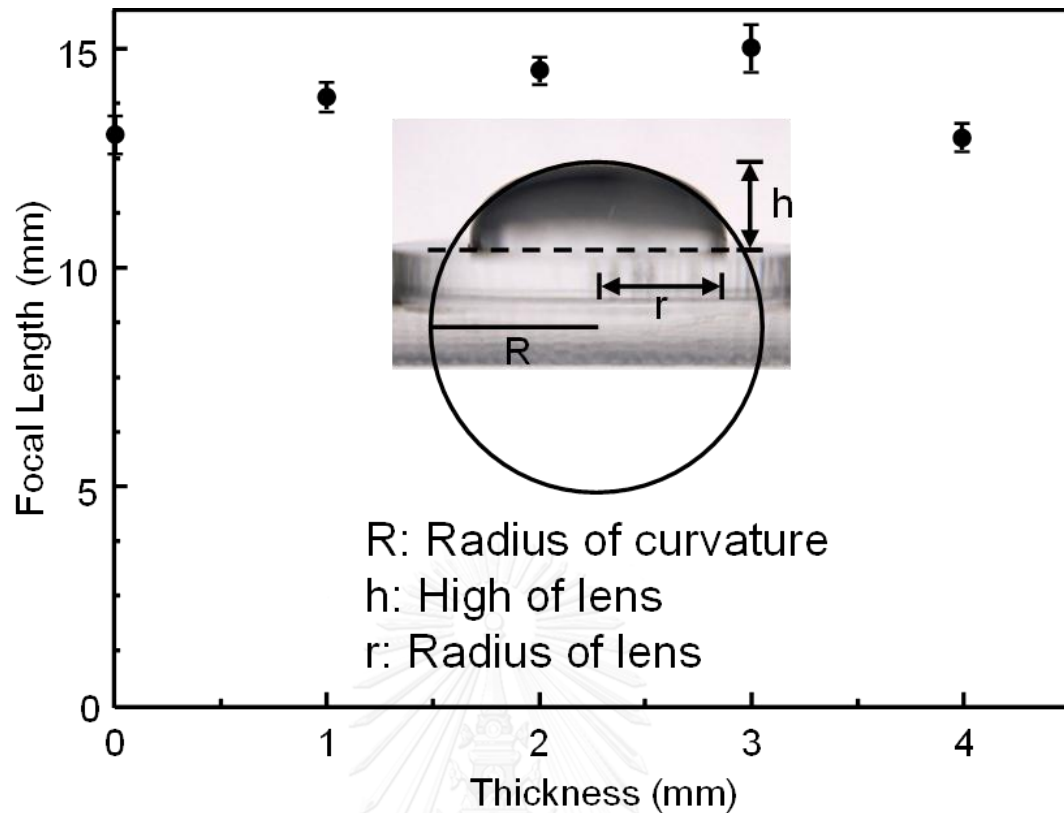


**Figure 4.12** Focal length of 6-mm PDMS elastomeric lens with base of different thickness. Based on the spherical cap fitting, the 6-mm lenses fabricated from a confined sessile drop of 40- $\mu$ L IPDMS have a radius of curvature  $R$  of 4.0 mm.

### 4.3 FIELD APPLICATIONS OF ePDMS PLANO-CONVEX LENSES

One particular promising application of the smartphone microscope is in the area of forensic science. Smartphone microscope is a novel tool that can efficiently assist the screening and collecting meaningful evidences. The compact and lightweight smartphone with high-resolution display, high pixel density optical sensor, long battery life, powerful processor, ease to use apps, and broadband internet

connection make the smartphone microscope an excellent imaging device for forensic analysis both in the field and in laboratory. The ePDMS elastomeric lens functioned as an external accessories interfacing with a smartphone in order to exploit its optical capabilities [33, 62]. Since the smartphone digital microscope is running on a battery, the microscopic investigation can be performed in the field without a restriction of electrical power supply. This unique advantage is very useful for samples or specimens that cannot be moved or transferred to a laboratory. Figure 4.13 show microscopic images of gun shot residue (GSR) on a cotton fabric generated by a point-blank shooting test. The images were taken at the shooting facility. GSRs on surface such as pillows, blankets, and cloths are common evidences. The GSRs invisible to the naked eyes can be clearly imaged with a high resolution microscope. In general, the whole pillow or blanket must be collected for thorough investigations in the lab. The bulky pillow form was taken out before GSR analysis. With a high magnification smartphone microscope, the GSR residues can be imaged without the removal of pillow form or the analysis can be performed on-site.

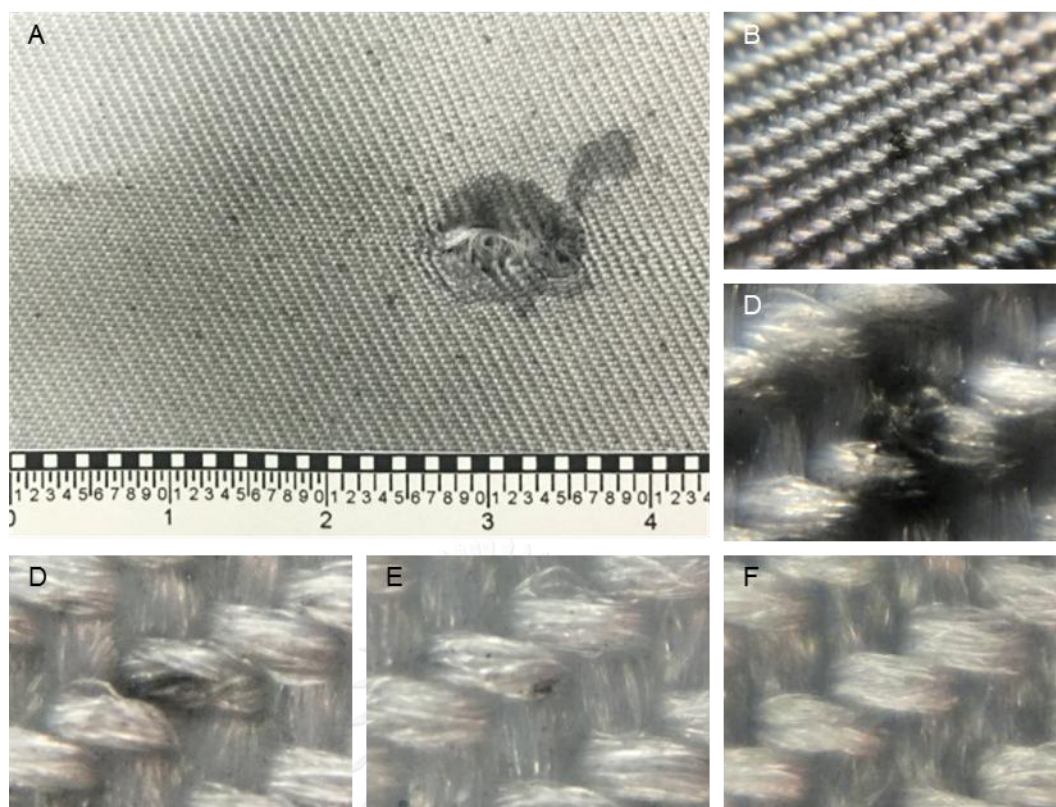


**Figure 4.13** (A) A photographic image of GSRs generate by a point-blank shooting on a cotton fabric. A microscopic image of a GSR taken by (B) normal photography and (C-E) 4X digital zoom. (F) A microscopic image of a clean cotton fabric. The microscope images were captured by an iPhone 6s Plus coupled with a 6-mm ePDMS plano-convex lens.

#### 4.4 PANORAMA MICROSCOPE IMAGING BY SMARTPHONE MICROSCOPE

In addition to high pixel density imaging, smartphones are equipped with powerful apps for video, slow motion, time-lapse, and panorama photography. Although those imbedded apps were designed for normal photography, they work equally well in the microscopic imaging. The panorama app with its powerful image-



stitching algorithm can unfold the detailed structural information on curved surface of a cylindrical object. The curved surface makes image analysis of cylindrical object more challenging. To explore the potential of smartphone panorama microscope for surface imaging of a small cylindrical object, we use paper strip (3.3 mm x 1.4 mm, Figure 4.15A) wrapping around a 10-mm cylinder as a model (Figure 4.15B). Due to a shallow depth-of-field of microscopic imaging, especially that at high magnification, microscopic images of the entire cylinder was not in focused (Figure 4.15C). However, by rotating the cylinder (i.e., by our homemade device) while taking photo under a panorama app of iPhone 6s Plus, the microscopic image of the cylindrical paper strip was reconstructed on-the-fly [69-74]. To trigger an image stitching, the entire image within the field of view must be moved. As a result, a smaller cylindrical object required lens with higher magnification. The microscopic panorama image was reconstructed in real-time during the rotation (Figure 4.14). Interestingly, the details of printed image as well as texture of the paper were efficiently captured without a detectable image distortion (Figure 4.15D). The high pixel density of the camera sensor enabled a graining-free digital zoom of the panorama microscope image. Although the microscope photography has shallow depth of field (Figure 4.15C), the panorama image is in focus without a detectable influence of the curved surface. The out-of-focus at the beginning and the end of the panorama image was due to the initial and final images used in the stitching algorithm [70-74].



**Figure 4.14** A series of still images show an experiment setup and panorama microscope imaging using a smartphone microscope equipped with a 5-mm ePDMS plano-convex lens and homemade rotating device. The device was rotated at 3 rpm while smartphone microscope taking panorama image of the 3.3 mm x 1.4 mm paper strip wrapped around a 10 mm cylinder. The panorama app stitched the images on-the-fly.



**Figure 4.15** Photographic images of a printed-paper strip as it: (A) was laid on a flat surface and (B) was wrapped around a 10 mm cylinder. (C) Microscopic images of the curved paper strip and (D) the corresponding panorama microscopic image of the curved paper strip taken by an iPhone 6s Plus coupled with a 3-mm lens (see Figure 4.14).

One of the challenging tasks in forensic analysis is the imaging of toolmarks on bullets. To demonstrate potential applications of panorama microscope imaging in toolmarks analysis, a 9-mm Luger bullets fired from a Glock 17 semi-automatic pistol was investigated. A full metal jacket (FMJ) bullet was fired into and retrieved from a Kevlar cast tube. The bullet was positioned on the rotating stage and imaged under the panorama app of an iPhone 6s Plus (Figure 4.16A). The panorama microscope image revealed detailed toolmarks on the surface of the bullet in a single photo (Figure 4.16C). The image did not show any sign of distortion and light reflection on the

curve surface. The normal microscopic images suffered from the reflection of the curved surfaces due to the illumination at the grazing angle of incidence (Figure 4.16B). Exact same patterns of toolmarks were observed while detail grooves of toolmarks on bullet surface were effectively captured in the panorama microscope image. To our knowledge, this is the first report on panorama microscope imaging using smartphone. The reconstructed panorama microscope images were distortion free. Due to the stitching algorithm, the curve surface appeared at the beginning and the end of the panorama image (Figures 4.15C and 4.16C). The microscope imaging and panorama microscope imaging by a smartphone can be applied to other applications that benefit from microscopic imaging. The smartphone microscope could drastically decrease the cost for microscopic investigation while making the point-of-care analysis widely available.

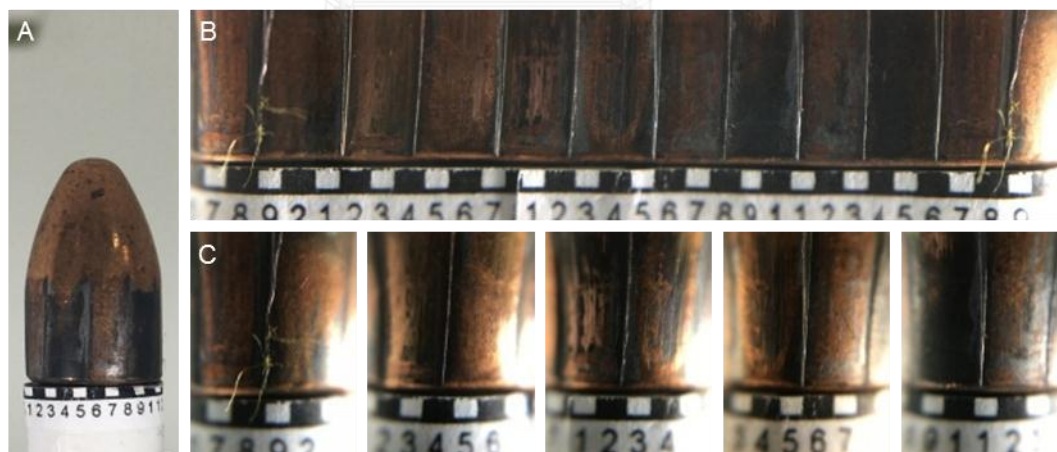
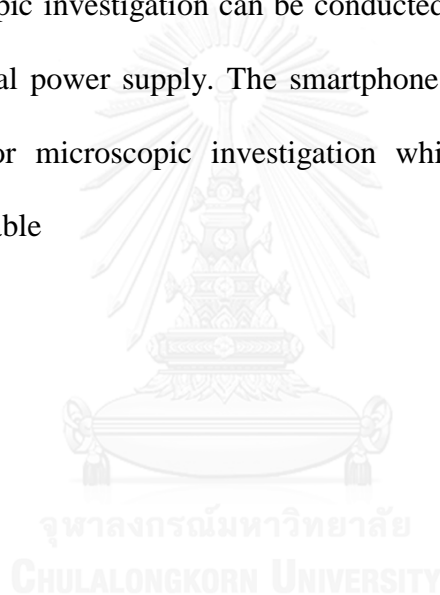


**Figure 4.16** (A) Photographic images of an FMJ bullet. (B) The corresponding microscopic images of the bullet and (C) panorama microscopic image of the bullet taken by an iPhone 6s Plus coupled with a 3-mm ePDMS plano-convex lens.

The mobile digital microscope equipped with ePDMS plano-convex lens exploits the state-of-the-art imaging capabilities of smartphone. The advance features of smartphone (i.e., lightweight, high-resolution display, high density optical sensor, long battery life, powerful processor, multi-platform wireless communication) made smartphone microscope highly mobile. The availability of low cost smartphone with high quality camera and advance image processing apps makes smartphone digital microscope more accessible and ease to use. Since smartphone is running on a battery, the microscopic investigation can be conducted anywhere anytime without a restriction of electrical power supply. The smartphone microscope could drastically decrease the cost for microscopic investigation while making the point-of-care analysis widely available



## CHAPTER V

### CONCLUSIONS

A simple, rapid, cost effective, and template-free technique for mass-scale production of ePDMS plano-convex lens of controllable size and focal length was successfully developed. By taking advantage of the resistance to spreading of liquid by a sharp edge, a stable spherical cap IPDMS with certain curvature and contact angle on a PMMA disk could be fabricated. A thermal treatment at 80 °C for 30 min cured the IPDMS into a bubble-free ePDMS plano-convex lens capable of turning a smartphone into a portable digital microscope. Elastomeric PDMS plano-convex lenses with focal lengths of 55.2-3.4 mm and magnifications of 4.5X-73.5X (without a digital zoom) could be reproducibly fabricated by dispensing 5-40  $\mu$ L IPDMS on 2-10 mm PMMA disks. The portable smartphone digital microscope could image small objects invisible to the naked eyes at high resolution. Applications of the portable smartphone digital microscope for imaging of micro-printing, gun shoot residue, and bullet toolmarks were demonstrated. High-resolution panorama microscope images without distortion of surfaces of cylindrical object can be reconstructed on-the-fly by an imbedded app.

## REFERENCES

1. Ahn, C. H.; Jin-Woo, C.; Beaucage, G.; Nevin, J. H.; Jeong-Bong, L.; Puntambekar, A.; Lee, J. Y., Disposable Smart Lab on a Chip for Point-of-Care Clinical Diagnostics. *Proceedings of the IEEE* **2004**, *92*, 154-173.
2. Bercich, R.; Bernhard, J.; Larson, K.; Lindsey, J., Hand-Held Plasma Isolation Device for Point-of-Care Testing. *IEEE Transactions on Biomedical Engineering* **2011**, *58*, 759-762.
3. Hersh, W.; Jacko, J. A.; Greenes, R.; Tan, J.; Janies, D.; Embi, P. J.; Payne, P. R. O., Health-Care Hit or Miss? *Nature* **2011**, *470*, 327-329.
4. Kazmierczak, S. C., Point-of-Care Testing Quality: Some Positives but Also Some Negatives. *Clinical Chemistry* **2011**, *57*, 1219-1220.
5. Myers, F. B.; Lee, L. P., Innovations in Optical Microfluidic Technologies for Point-of-Care Diagnostics. *Lab on a Chip* **2008**, *8*, 2015-2031.
6. Pollock, N. R.; Rolland, J. P.; Kumar, S.; Beattie, P. D.; Jain, S.; Noubary, F.; Wong, V. L.; Pohlmann, R. A.; Ryan, U. S.; Whitesides, G. M., A Paper-Based Multiplexed Transaminase Test for Low-Cost, Point-of-Care Liver Function Testing. *Science Translational Medicine* **2012**, *4*, DOI: 10.1126/scitranslmed.3003981.
7. Wang, E.; Meier, D. J.; Sandoval, R. M.; Hendy-Willson, V. E. V.; Pressler, B. M.; Bunch, R. M.; Alloosh, M.; Sturek, M. S.; Schwartz, G. J.; Molitoris, B. A., A Portable Fiberoptic Ratiometric Fluorescence Analyzer Provides Rapid Point-of-Care Determination of Glomerular Filtration Rate in Large Animals. *Kidney International* **2012**, *81*, 112–117.

8. Wang, S.; Xu, F.; Demirci, U., Advances in developing HIV-1 viral load assays for resource-limited settings. *Biotechnology Advances* **2010**, *28*, 770-781.
9. Xu, X.; Akay, A.; Wei, H.; Wang, S.; Pinguan-Murphy, B.; Erlandsson, B. E.; Li, X.; Lee, W.; Hu, J.; Wang, L.; Xu, F., Advances in Smartphone-Based Point-of-Care Diagnostics. *Proceedings of the IEEE* **2015**, *103*, 236-247.
10. Duffy, D. C.; McDonald, J. C.; Schueller, O. J. A.; Whitesides, G. M., Rapid Prototyping of Microfluidic Systems in Poly(dimethylsiloxane). *Analytical chemistry* **1998**, *70*, 4974-4984.
11. Lillehoj, P. B.; Huang, M.-C.; Truong, N.; Ho, C.-M., Rapid Electrochemical Detection on a Mobile Phone. *Lab on a Chip* **2013**, *13*, 2950-2955.
12. Ericsson Mobility Report. <http://www.ericsson.com/res/docs/2015/mobility-report/ericsson-mobility-report-nov-2015.pdf> (accessed April 3, 2016).
13. Ansari, N.; Lodha, A.; Pandya, A.; Sutariya, P. G.; Menon, S. K., Lab-on-Phone Citrate-Capped Silver Nanosensor for Lidocaine Hydrochloride Detection from a Biological Matrix. *Analytical Methods* **2015**, *7*, 9084-9091.
14. Berg, B.; Cortazar, B.; Tseng, D.; Ozkan, H.; Feng, S.; Wei, Q.; Chan, R. Y.-L.; Burbano, J.; Farooqui, Q.; Lewinski, M.; Di Carlo, D.; Garner, O. B.; Ozcan, A., Cellphone-Based Hand-Held Microplate Reader for Point-of-Care Testing of Enzyme-Linked Immunosorbent Assays. *ACS Nano* **2015**, *9*, 7857-7866.
15. Bueno, L.; Cottell, A.; Reddy, S. M.; Paixao, T. R. L. C., Coupling Dye-Integrated Polymeric Membranes with Smartphone Detection to Classify Bacteria. *RSC Advances* **2015**, *5*, 97962-97965.



16. Kwok, D. Y.; Neumann, A. W., Contact Angle Measurement and Contact Angle Interpretation. *Advances in colloid and interface science* **1999**, *81*, 167-249.
17. Laksanasopin, T.; Guo, T. W.; Nayak, S.; Sridhara, A. A.; Xie, S.; Olowookere, O. O.; Cadinu, P.; Meng, F.; Chee, N. H.; Kim, J.; Chin, C. D.; Munyazes, E.; Mugwaneza, P.; Rai, A. J.; Mugisha, V.; Castro, A. R.; Steinmiller, D.; Linder, V.; Justman, J. E.; Nsanzimana, S.; Sia, S. K., A smartphone Dongle for Diagnosis of Infectious Diseases at the Point of Care. *Science Translational Medicine* **2015**, *7*, DOI: 10.1126/scitranslmed.aaa0056.
18. Liang, P.-S.; Park, T. S.; Yoon, J.-Y., Rapid and Reagentless Detection of Microbial Contamination Within Meat Utilizing a Smartphone-Based Biosensor. *Scientific reports* **2014**, *4*, DOI: 10.1038/srep05953.
19. Ozcan, A., Mobile Phones Democratize and Cultivate Next-Generation Imaging, Diagnostics and Measurement Tools. *Lab on a Chip* **2014**, *14*, 3187-3194.
20. Wei, Q.; Qi, H.; Luo, W.; Tseng, D.; Ki, S. J.; Wan, Z.; Göröcs, Z.; Bentolila, L. A.; Wu, T.-T.; Sun, R.; Ozcan, A., Fluorescent Imaging of Single Nanoparticles and Viruses on a Smart Phone. *ACS Nano* **2013**, *7*, 9147-9155.
21. Wu, T. F.; Qiao, W.; Chiu, Y. J.; Lo, Y. H., 9 - Optofluidic lab-on-a-chip devices for photomedicine applications. In *Applications of Nanoscience in Photomedicine*, Chandos Publishing: Oxford, **2015**, pp 169-184.
22. Campos, A. R.; Knutson, C. M.; Knutson, T. R.; Mozzetti, A. R.; Haynes, C. L.; Penn, R. L., Quantifying Gold Nanoparticle Concentration in a Dietary

- Supplement Using Smartphone Colorimetry and Google Applications. *Journal of Chemical Education* **2016**, *93*, 318-321.
23. Grasse, E. K.; Torcasio, M. H.; Smith, A. W., Teaching UV–Vis Spectroscopy with a 3D-Printable Smartphone Spectrophotometer. *Journal of Chemical Education* **2016**, *93*, 146-151.
24. Long, K. D.; Yu, H.; Cunningham, B. T., Smartphone Instrument for Portable Enzyme-Linked Immunosorbent Assays. *Biomedical optics express* **2014**, *5*, 3792-3806.
25. Yu, H.; Tan, Y.; Cunningham, B. T., Smartphone Fluorescence Spectroscopy. *Analytical chemistry* **2014**, *86*, 8805-8813.
26. Zhang, C.; Cheng, G.; Edwards, P.; Zhou, M.-D.; Zheng, S.; Liu, Z., G-Fresnel smartphone spectrometer. *Lab on a Chip* **2016**, *16*, 246-250.
27. Chan, H. N.; Shu, Y.; Xiong, B.; Chen, Y.; Chen, Y.; Tian, Q.; Michael, S. A.; Shen, B.; Wu, H., Simple, Cost-Effective 3D Printed Microfluidic Components for Disposable, Point-of-Care Colorimetric Analysis. *ACS Sensors* **2016**, *1*, 227-234.
28. Dutta, S.; Saikia, K.; Nath, P., Smartphone based LSPR sensing platform for bio-conjugation detection and quantification. *RSC Advances* **2016**, *6*, 21871-21880.
29. Guan, L.; Tian, J.; Cao, R.; Li, M.; Cai, Z.; Shen, W., Barcode-Like Paper Sensor for Smartphone Diagnostics: An Application of Blood Typing. *Analytical chemistry* **2014**, *86*, 11362-11367.
30. Gunda, N. S. K.; Naicker, S.; Shinde, S.; Kimbahune, S.; Shrivastava, S.; Mitra, S., Mobile Water Kit (MWK): A Smartphone Compatible Low-Cost

Water Monitoring System for Rapid Detection of Total Coliform and E. Coli. *Analytical Methods* **2014**, *6*, 6236–6246.

31. Kim, K. Y.; Park, S.; Jung, S. H.; Lee, S. S.; Park, K.-M.; Shinkai, S.; Jung, J. H., Geometric Change of a Thiocalix[4]arene Supramolecular Gel with Volatile Gases and Its Chromogenic Detection for Rapid Analysis. *Inorganic chemistry* **2014**, *53*, 3004-3011.
32. Breslauer, D. N.; Maamari, R. N.; Switz, N. A.; Lam, W. A.; Fletcher, D. A., Mobile Phone Based Clinical Microscopy for Global Health Applications. *PLoS ONE* **2009**, *4*, DOI: 10.1371/journal.pone.0006320.g0006001.
33. Phillips, Z. F.; D'Ambrosio, M. V.; Tian, L.; Rulison, J. J.; Patel, H. S.; Sadras, N.; Gande, A. V.; Switz, N. A.; Fletcher, D. A.; Waller, L., Multi-Contrast Imaging and Digital Refocusing on a Mobile Microscope with a Domed LED Array. *PLoS ONE* **2015**, *10*, DOI: 10.1371/journal.pone.0124938.
34. Switz, N. A.; D'Ambrosio, M. V.; Fletcher, D. A., Low-Cost Mobile Phone Microscopy with a Reversed Mobile Phone Camera Lens. *PLoS ONE* **2014**, *9*, DOI: 10.1371/journal.pone.0095330.
35. Smith, Z. J.; Chu, K.; Espenson, A. R.; Rahimzadeh, M.; Gryshuk, A.; Molinaro, M.; Dwyre, D. M.; Lane, S.; Matthews, D.; Wachsmann-Hogiu, S., Cell-Phone-Based Platform for Biomedical Device Development and Education Applications. *PLoS ONE* **2011**, *6*, DOI: 10.1371/journal.pone.0017150.
36. D'Ambrosio, M. V.; Bakalar, M.; Bennuru, S.; Reber, C.; Skandarajah, A.; Nilsson, L.; Switz, N.; Kamgno, J.; Pion, S.; Boussinesq, M.; Nutman, T. B.; Fletcher, D. A., Point-of-Care Quantification of Blood-Borne Filarial Parasites

- with a Mobile Phone Microscope. *Science Translational Medicine* **2015**, *7*, DOI: 10.1126/scitranslmed.aaa3480.
37. Lee, W. M.; Upadhyaya, A.; Reece, P. J.; Phan, T. G., Fabricating Low Cost and High Performance Elastomer Lenses Using Hanging Droplets. *Biomedical optics express* **2014**, *5*, 1626-1635.
  38. McDonald, C.; McGloin, D., Low-Cost Optical Manipulation Using Hanging Droplets of PDMS. *RSC Advances* **2015**, *5*, 55561-55565.
  39. Zeng, X.; Jiang, H., Polydimethylsiloxane Microlens Arrays Fabricated Through Liquid-Phase Photopolymerization and Molding. *Journal of Microelectromechanical Systems* **2008**, *17*, 1210-1217.
  40. Chapman, M. W.; Langlois, J. P.; Thoni, M. A. Portable Electronic Device Case Accessory with Interchangeable Camera Lens System. US 20130177304A1, **July 11, 2013**.
  41. O'Neill, P. D. Lenses for Communication Devices. US 8593745B2, **November 26, 2013**.
  42. Pirstill, C. W.; Coté, G. L., Malaria Diagnosis Using a Mobile Phone Polarized Microscope. *Scientific reports* **2015**, *5*, DOI: 10.1038/srep13368.
  43. Sung, Y.-L.; Jeang, J.; Lee, C.-H.; Shih, W.-C., Fabricating optical lenses by inkjet printing and heat-assisted in situ curing of polydimethylsiloxane for smartphone microscopy. *Journal of Biomedical Optics* **2015**, *20*, 047001-047006.
  44. Evenou, F.; Fujii, T.; Sakai, Y., Liver Cells Culture on Three-Dimensional Micropatterned Polydimethylsiloxane Surfaces. In *6th World Congress on*

*Alternatives & Animal Use in the Life Sciences*, August 21-25, 2007, Tokyo, Japan, **2007**; Vol. 14, pp 665-668.

45. Seethapathy, S.; Górecki, T., Applications of Polydimethylsiloxane in Analytical Chemistry: A Review. *Analytica Chimica Acta* **2012**, *750*, 48-62.
46. Lisensky, G. C.; Campbell, D. J.; Beckman, K. J.; Calderon, C. E.; Doolan, P. W.; Rebecca, M. O.; Ellis, A. B., Replication and Compression of Surface Structures with Polydimethylsiloxane Elastomer. *Journal of Chemical Education* **1999**, *76*, 537-541.
47. Cruz Félix, A. S.; Santiago-Alvarado, A.; Iturbide-Jiménez, F.; Licona-Morán, B., Physical-Chemical Properties of PDMS Samples Used in Tunable Lenses. *International Journal of Engineering Science and Innovative Technology* **2014**, *3*, 563-571.
48. Ren, H.; Wu, S.-T., *Introduction to Adaptive Lenses*. Wiley: USA, **2012**; p 286.
49. Shih, T.-K.; Chen, C.-F.; Ho, J.-R.; Chuang, F.-T., Fabrication of PDMS (polydimethylsiloxane) microlens and diffuser using replica molding. *Microelectronic Engineering* **2006**, *83*, 2499-2503.
50. Cruz-Campa, J. L.; Okandan, M.; Busse, M. L.; Nielson, G. N., Microlens Rapid Prototyping Technique with Capability for Wide Variation in Lens Diameter and Focal Length. *Microelectronic Engineering* **2010**, *87*, 2376-2381.
51. Hsieh, H.-T.; Lin, V.; Hsieh, J.-L.; Su, G.-D. J., Design and Fabrication of Long Focal Length Microlens Arrays. *Optics Communications* **2011**, *284*, 5225-5230.

52. Wang, Y.-C.; Tsai, Y.-C.; Shih, W.-P., Flexible PDMS micro-lens array with programmable focus gradient fabricated by dielectrophoresis force. *Microelectronic Engineering* **2011**, *88*, 2748-2750.
53. Wong, E. J. Modeling and Control of Rapid Cure in Polydimethylsiloxane (PDMS) for Microfluidic Device Applications. PhD Thesis, Massachusetts Institute of Technology, **2010**.
54. Oliver, J. F.; Huh, C.; Mason, S. G., Resistance to Spreading of Liquids by Sharp Edges. *Journal of Colloid and Interface Science* **1977**, *59*, 568-581.
55. Hoheisel, D.; Kelb, C.; Wall, M.; Roth, B.; Rissing, L., Fabrication of Adhesive Lenses Using Free Surface Shaping. *Journal of the European Optical Society Rapid Publications* **2013**, *8*, 1990-2573.
56. Amarit, R.; Kopwitthaya, A.; Pongsoon, P.; Jarujareet, U.; Chaitavon, K.; Porntheeraphat, S.; Sumriddetchkajorn, S.; Koanantakool, T., High-Quality Large-Magnification Polymer Lens from Needle Moving Technique and Thermal Assisted Moldless Fabrication Process. *PLoS One* **2016**, *11*, DOI: 10.1371/journal.pone.0146414.
57. Roda, A.; Michelini, E.; Zangheri, M.; Di Fusco, M.; Calabria, D.; Simoni, P., Smartphone-Based Biosensors: A Critical Review and Perspectives. *TrAC Trends in Analytical Chemistry* **2015**, *79*, DOI: 10.1016/j.trac.2015.1010.1019.
58. Bayramli, E.; Mason, S. G., Liquid Spreading: Edge Effect for Zero Contact Angle. *Journal of Colloid and Interface Science* **1978**, *66*, 200–202.
59. Wilbur, J. L.; Jackman, R. J.; Whitesides, G. M.; Cheung, E. L.; Lee, L. K.; Prentiss, M. G., Elastomeric Optics. *Chemistry of Materials* **1996**, *8*, 1380-1385.

60. Fang, G.; Amirfazli, A., Understanding the Edge Effect in Wetting: a Thermodynamic Approach. *Langmuir : the ACS journal of surfaces and colloids* **2012**, *28*, 9421–9430.
61. Schneider, F.; Draheim, J.; Kamberger, R.; Wallrabe, U., Process and Material Properties of Polydimethylsiloxane (PDMS) for Optical MEMS. *Sensors and Actuators A: Physical* **2009**, *151*, 95–99.
62. Toth, T.; Ferraro, D.; Chiarello, E.; Pierno, M.; Mistura, G.; Bissacco, G.; Semperebon, C., Suspension of Water Droplets on Individual Pillars. *Langmuir : the ACS journal of surfaces and colloids* **2011**, *27*, 4742–4748.
63. Cybulski, J. S.; Clements, J.; Prakash, M., Foldscope: Origami-Based Paper Microscope. *PLoS One* **2014**, *9*, DOI: 10.1371/journal.pone.0098781.g0098001.
64. Larson, T. E. Surface Adhering Lens. US 20140362239A1, **December 1 1, 2014**.
65. Das, A. K.; Das, P. K., Equilibrium Shape and Contact Angle of Sessile Drops of Different volumes—Computation by SPH and its Further Improvement by DI. *Chemical Engineering Science* **2010**, *65*, 4027-4037.
66. Harry, A.; Janet Qi Zhou; Yann Gambin; Stephen R. Quake Nonimaging Concentrator Lens Arrays and Microfabrication of the Same. US 6804062 B2, **October 12, 2004**.
67. Lee, S. A.; Yang, C., A smartphone-Based Chip-Scale Microscope Using Ambient Illumination. *Lab Chip* **2014**, *14*, 3056–3063.

68. Stroppa, D. G.; Unfried S., J.; Hermenegildo, T.; Ramirez, A. J., Measuring Contact Angles on Sessile Drop Test Samples. *Welding Journal* **2010**, *89*, 47–49.
69. Vafaei, S.; Podowski, M. Z., Analysis of the Relationship Between Liquid Droplet Size and Contact Angle. *Advances in colloid and interface science* **2005**, *113*, 133–146.
70. Bhogal, N.; Doepke, F. Panorama Processing. US 20120293607 A1, **November 22, 2012**.
71. Daponte, P.; De Vito, L.; Picariello, F.; Riccio, M., State of the Art and Future Developments of the Augmented Reality for Measurement Applications. *Measurement* **2014**, *57*, 53–70.
72. Doepke, F. Positional Sensor-Assisted Image Registration for Panoramic Photography. US 8600194 B2, **December 3, 2013**.
73. Doepke, F.; Brunner, R. Intelligent image Blending for Panoramic Photography. US 9088714 B2, **November 22, 2012**.
74. Vafaei, S.; Podowski, M. Z., Theoretical Analysis on the Effect of Liquid Droplet Geometry on Contact Angle. *Nuclear Engineering and Design* **2005**, *235*, 1293–1301.





**APPENDIX**

จุฬาลงกรณ์มหาวิทยาลัย  
CHULALONGKORN UNIVERSITY

## Elastomeric PDMS Planoconvex Lenses Fabricated by a Confined Sessile Drop Technique

S. Ekgasit,<sup>\*,†</sup> N. Kaewmanee,<sup>†</sup> P. Jangtawee,<sup>†</sup> C. Thammacharoen,<sup>†</sup> and M. Donphoongpri<sup>‡</sup>

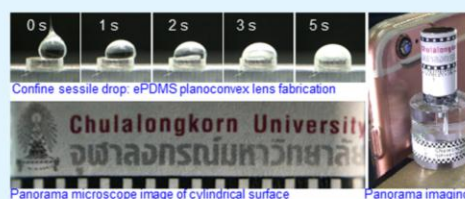
<sup>†</sup>Sensor Research Unit, Department of Chemistry, Faculty of Science, Chulalongkorn University, 254 Phayathai Road, Patumwan, Bangkok 10330, Thailand

<sup>‡</sup>Central Institute of Forensic Science (CIFS), 8th Floor, B Building, The Government Complex, Chaengwattana Road, Laksi, Bangkok 10210 Thailand

### Supporting Information

**ABSTRACT:** The ubiquity of high quality smartphones at affordable prices not only accelerated the social penetration in the global population but also promoted nontraditional usage of smartphones as point-of-care medical diagnostic devices, sensors, and portable digital microscopes. This paper reveals a simple, rapid, cost-effective, and template-free technique for mass-scale production of an elastomeric PDMS (ePDMS) planoconvex lens capable of converting a smartphone into a portable digital microscope. By taking advantage of the resistance to spreading of liquid by a sharp edge, highly stable spherical cap of viscous liquid PDMS (IPDMS) on a smooth PMMA circular disk was fabricated. The axisymmetric spreading of IPDMS under the gravitational force and interfacial tension force enable the formation of spherical cap with a certain radius of curvature. A thermal treatment at 80 °C for 30 min cured the spherical cap IPDMS into a bubble-free ePDMS planoconvex lens. Lenses with focal lengths of 55.2–3.4 mm could be reproducibly fabricated by adjusting the volume of dispensed IPDMSs and diameter of PMMA disks. High-resolution panoramic microscope images without a distortion of small cylindrical object could be constructed on-the-fly using the imbedded smartphone app. Applications of the smartphone digital microscope equipped with an ePDMS planoconvex lens for imaging of micro printings, gun shot residues, cylindrical objects, and bullet toolmarks were explored.

**KEYWORDS:** PDMS lens, smartphone microscope, sessile drop, Gibbs inequality condition, spreading resistance



### 1. INTRODUCTION

The worldwide availability of compact and lightweight smartphones with powerful processors, high quality displays, large volume storage, connectivity (3G, 4G, Wi-Fi, bluetooth, near field communication), ease to use apps, and state-of-the-art sensors (camera, proximity sensor, magnetometer, accelerometer, gyroscope, microphone, fingerprint sensor, thermometer, and light sensor) at affordable prices make smartphones the future point-of-care devices. There were 87 million new global subscriptions of mobile phones in the third quarter of 2015 alone. At the end of 2015, the number of mobile phone subscriptions was greater than that of the global population with a greater number of smartphone subscriptions compared to that of the basic phones.<sup>1</sup>

Lab-on-phone devices that take advantage of smartphone functionalities as biosensors,<sup>2–10</sup> spectrometer,<sup>11–14</sup> and colorimetric sensors<sup>15–20</sup> have been fabricated. Powerful image processing with high pixel density image sensors encouraged researchers to explore its potential as an affordable mobile digital microscope capable of capturing and sharing detailed microscopic images anywhere, anytime by attaching an external lens onto the smartphone camera. Various types of lenses including objective lens,<sup>21–23</sup> ball lens,<sup>23,24</sup> planoconvex lens,<sup>9</sup> iPhone lens module,<sup>23–25</sup> PDMS elastomeric lens,<sup>26–29</sup>

and microscope lens<sup>30–32</sup> were employed for coupling the magnified image into the optical system of the smartphone without a hardware modification. The image quality and magnification are strongly dependent on the lens and attachment design. Smartphone microscope images with resolutions of 1.2  $\mu\text{m}$  by an objective lens,<sup>21</sup> 1.5  $\mu\text{m}$  by a planoconvex lens,<sup>9</sup> 1.5  $\mu\text{m}$  by a ball lens,<sup>24</sup> 1.1  $\mu\text{m}$  by a PDMS elastomeric lens,<sup>28</sup> and 3.9  $\mu\text{m}$  by a hanging drop PDMS elastomeric lens<sup>26</sup> were successfully acquired.

Due to its optical transparency from UV to NIR regions and nonfluorescence property, optical grade liquid polydimethylsiloxane (IPDMS: Sylgard 184 from Dow Corning and RTV 615 from Bayer Silicones) has been used for elastomeric optics (lenses, mirrors, and gratings), microfluidic devices, and microelectromechanic system (MEMS) fabrications. PDMS elastomer is highly chemically resistant and inert. It can withstand dimensional alteration (compression or expansion) without losing or degrading optical properties. A thermal curing at moderate temperature (80–200 °C) enables rapid fabrication of planoconvex PDMS elastomeric lenses for

Received: May 26, 2016

Accepted: July 15, 2016

Published: July 15, 2016

## VITA

**Name:** Miss Natthanan Kaewmanee  
**Date of birth:** January 6, 1991  
**Birth place:** Songkhla, Thailand  
**Address:** 121 Khao Rupchang, Muang, Songkhla 90000, Thailand

### University Education:

2013 B. Sc. (Polymeric Science) Prince of Songkla University, Songkhla, Thailand

### Conference Presentations:

"Fabrication of Smartphone Compatible PDMS Elastomer Lens having Precisely Controlled Focal Length Using Constrained Sessile Drop Casting Technique" at Pure and Applied Chemistry International Conference 2016 (PACCON 2016) in Bangkok, Thailand, February 9-11, 2016

"Fabrication of PDMS Plano-convex Lenses with Precisely Controlled Curvatures by Confined Sessile Drop Technique" at The International Polymer Conference of Thailand 2016 (PCT-6) in Bangkok, Thailand, June 30 - July 1, 2016

### Publication:

Ekgasit, S.; Kaewmanee, N.; Jangtawee, P.; Thammacharoen, C.; Donphongpri, M., Elastomeric PDMS Planoconvex Lenses Fabricated by a Confined Sessile Drop Technique. *ACS Applied Materials & Interfaces* **2016**, 8, 20474-20482.

**Award:**

2016 Honorable mention award in Sci & Tech Initiative and Sustainability

Awards 9<sup>th</sup>



